SECURITY CLASSIFICATION OF THIS PAGE *(When Data Entered)*

REPORT DOCUMENTATION PAGE

READ INSTRUCTIONS BEFORE COMPLETING FORM

1. REPORT NUMBER: AFWAL-TR-80-4136	2. GOVT ACCESSION NO.
3. RECIPIENT'S CATALOG NUMBER	
4. TITLE *(and Subtitle)* AN EXPERIMENTAL EVALUATION OF THE MECHANICAL RESPONSE CHARACTERISTICS OF RENE 95	5. TYPE OF REPORT & PERIOD COVERED: Interim Report for Period Sept. 1978-Apr. 1980
	6. PERFORMING ORG. REPORT NUMBER
7. AUTHOR(s) D.C. Stouffer and L. Papernik, Dept. Engr. Science, Univ. Cincinnati, Cinti., Ohio. H.L. Bernstein, Systems Research Laboratory, Dayton, Ohio	8. CONTRACT OR GRANT NUMBER(s): F33615-78-C 5199
9. PERFORMING ORGANIZATION NAME AND ADDRESS	10. PROGRAM ELEMENT, PROJECT, TASK AREA & WORK UNIT NUMBERS: 2307P110
11. CONTROLLING OFFICE NAME AND ADDRESS: Materials Laboratory (AFWAL/MLLN) Air Force Wright Aeronautical Laboratory (AFSC) Wright Patterson Air Force Base, Ohio 45433	12. REPORT DATE: October, 1980 13. NUMBER OF PAGES: 68
14. MONITORING AGENCY NAME & ADDRESS *(if different from Controlling Office)*	15. SECURITY CLASS. *(of this report)*: Unclassified 15a. DECLASSIFICATION/DOWNGRADING SCHEDULE

16. DISTRIBUTION STATEMENT *(of this Report)*

Approved for Public Release; Distribution Unlimited.

17. DISTRIBUTION STATEMENT *(of the abstract entered in Block 20, if different from Report)*

18. SUPPLEMENTARY NOTES

19. KEY WORDS *(Continue on reverse side if necessary and identify by block number)*

RENE 95
Mechanical Properties
Creep
Sress Relaxation
Recovery
Fatigue
Strain Rate Effects

20. ABSTRACT *(Continue on reverse side if necessary and identify by block number)*

The mechanical responses of thermomechanically processed cast and wrought René 95 at 650°C (1200°F) was studied. The experimental program included: tensile and compressive tests at different constant strain rates, creep in tension at and compression at twelve stress levels, strain recovery, stress

DD FORM 1 JAN 73 1473 EDITION OF 1 NOV 65 IS OBSOLETE

SECURITY CLASSIFICATION OF THIS PAGE *(When Data Entered)*

relaxation, creep response to a sequence of step stress histories and fatigue under load control.

The results are important for the understanding of the material response characteristics and for the development of a realistic constitutive model. Most of the tests were done in tension and data was used to evaluate various constitutive assumptions.

It was shown that the engineering stress-strain response is relatively insensitive to changes in strain rate at rates above 5%/min. It was also shown that the compressive stress-strain response is about 10% stiffer than the tensile response and the minimum creep rate in tension is about one decade faster than the corresponding creep rate in compression. The hysteresis loop developed a mean tensile strain. It was found that the logarithm of the minimum creep rate is linear in the true stress and that creep and stress relaxation can be correlated using isochronous creep curves. The minimum creep rate is also independent of step changes in the stress history.

Foreword

This Technical Report was prepared by the Department of Aerospace Engineering and Applied Mechanics of the University of Cincinnati. Dr. T. Nicholas, AFWAL/MLLN was the project engineer. This report describes the results of the experimental program on René 95 at 650°C and is the completion of Tasks 4.2.2 and 4.2.4 of Contract F33615-78-C-5199, "Constitutive Modeling". The research reported was conducted by D. C. Stouffer, L. Papernik and H. L. Bernstein from September 1978 to April 1980. The report was submitted for publication in June 1980.

The authors express the appreciation to Dr. T. Nicholas for his suggestions and comments during the project. The authors gratefully acknowledge the work of Metcut Research Associates, Inc., Cincinnati, Ohio, for the machining of the specimens, and the General Electric Company of Evendale, Ohio, for their cooperation in the specimen manufacture. The authors express sincere thanks to Joe Conway and Ray Stentz of Mar-Test, Inc., Cincinnati, Ohio, for their many discussions in the analysis of the data; and, the entire Mar-Test staff for their assistance in running the experimental program. Finally, the authors are indebted to Vivek Rao and Kulwant Virdi for reducing the data and developing the plotter programs to produce the curves displayed in this document.

TABLE OF CONTENTS

LIST OF ILUSTRATIONS

LIST OF ILLUSTRATION (Concluded)

LIST OF TABLES

SECTION I
INTRODUCTION

The modern design of gas turbines has emphasized high performance and high thrust/weight ratios, resulting in higher stresses and temperatures on rotating components. Combined with the increased requirements for longer service life, this necessitates the development of accurate constitutive models capable of fully characterizing the deformation behavior of the material under different load histories that closely simulate the real working conditions of the material in service. This involves an interaction of a number of effects, such as strain hardening, creep, fatigue, stress-relaxation and strain-recovery at elevated temperatures. In turn, the successful constitutive modeling depends, to a great extent, on a well established experimental program that provides all the necessary information for obtaining the response characteristics of the material.

In recent years advanced nickel base super alloys have been introduced for use in jet engines. One such material is thermomechanically processed (TMP) cast and wrought René 95. A number of studies of the microstructure of René 95 were made (Reference 1-4). It is generally accepted that TMP René 95 has a duplex microstructure consisting of large warm worked grains surrounded by a grain boundary with fine recrystallized grains. It has been shown that the presence of MC carbides enhances creep resistance but reduces the performance by enhancing crack initiation which leads to shorter lives in low cycle fatigue tests (Reference 5).

Subsequently, the low cycle fatigue behavior of René 95 was studied. Based on a limited number of tests, Menon concluded that creep damage had little effect on the low cycle fatigue behavior (Reference 6). However, Bernstein showed that the creep-fatigue characteristics of René 95 are quite complicated (Reference 7). In a recent report, he concluded that the fatigue

life of René 95 could not be adequately predicted by four of the models frequently used in the literature (Reference 8-17). In a preliminary study (Reference 18) to establish the monotonic response properties of René 95, it was shown that fatigue damage appears to effect the primary creep but has little effect on the minimum creep rate. This was unexpected since Plumbridge and Miller (Reference 19) observed an increase in the minimum creep rate due to prior fatigue in 1 Cr-Mo-V steel at 565°C. The data from (Reference 18) was also used to develop the constants in the Bodner-Partom Equation (Reference 20, 21), however, the predictive capability of the model was partially limited due to the inaccuracies in the experimental data.

These reports, showing a mixed set of properties, clearly indicate the need for a complete and comprehensive study of the mechanical response properties of René 95 for development of constitutive equations. The experimental program described in this report evaluated the following response properties:

(a) The stress response due to strain in tension and compression at different constant strain rates.

(b) The creep response in tension and compression at different constant load histories.

(c) The change in the tensile creep response due to small changes in temperature from 650°C. (1200°F.)

(d) The effect of step changes in the stress history on the minimum creep rate.

(e) The stress relaxation response to different constant strain histories.

(f) The strain recovery at near zero stress after constant stress and constant strain rate histories.

(g) The strain response to stress in tension at different constant load rate histories.

(h) The cyclic fatigue response under load control.

(i) The effect of prior creep damage on the low cycle fatigue properties.

All experiments were run on cast and wrought TMP René 95 at 650°C. (1200°F). The same equipment and specimen geometry was used for all experiments in an attempt to guarantee repeatability. Since the life of superalloys of this type are generally controlled by load rather than strain (Reference 22), load control was chosen over strain control in many experiments for the potential convenience in correlating failure data. The total strain, inelastic strain and load histories were recorded in most experiments. These data are the basis of the current report.

SECTION II
DESCRIPTION OF THE MATERIAL

Renè 95 is a nickel-base super alloy, normally available as forging (pancake) plate and bar, with primary usage in jet engine turbine disks. The strength of Renè 95 at temperatures between 700°F and 1200°F. is significantly higher than most commercially available alloys.

The nominal chemical composition of Renè 95 is given in Table 1, with specification limits. The alloy is strengthened by a combination of gamma prime precipitation Ni_3, (Al, Ti, Cb) , solid solution lattice-strain, and thermomechanical processing to obtain a good balance between strength and ductility. The total percentage weight of the elements forming the gamma prime (Al, Ti, and Cb) is 9.5; the number from which the alloy derives its name.

The pancake of Renè 95 used in this program was taken from a vacuum induction melted and vacuum arc remelted ingot approximately 0.228m in diameter. The ingot was given a homogenization anneal in the range 1163-1190°C (2125-2175° F) for three hours and then furnace cooled. The pancake was subseqently reheated to 1093-1138°C (2000-2080°F) and forged to bring the thickness to 40-50% above the final value. This was followed by a recrystallization at 1163°C ± 14°C (2125°F ± 25°F) for one hour. This resulted in a uniform grain diameter between 0.064 to 0.127 mm. The forging was cooled from the recrystallization temperature at a rate greater than 83°C (150°F) per hour to 899°C (1650°F) and then air cooled for final processing. The forgings were reheated to 1079-1107°C (1975-2025°F) and the final reduction was applied, resulting in a further 40-50% decrease in thickness. The pancakes were then oil quenched and aged. The final size of the pancake was 38 cm (15 inches) in diameter and 4.50 cm (1.75 inches) thick as shown in Figure 1.

The thermomechanical processing produces a duplex structure in which large warm worked grains are surrounded by a "necklace" of fine recrystallized grains (see Figure 2a). In addition to the uniform distribution of the gamma prime precipitate, the material derives part of its strength from the extensive residual dislocation substructure in the warm worked grains. Contrary to Menon (Reference 6), we did find significant variation in the grain size and shape with variation in radial direction (compare Figure 2b to Figure 2a). However, due to the extensive dislocation substructure in all warm worked grains, variation in the macroscopic properties of the material negligible unless failure occurs at the grain boundaries.

To minimize the macroscopic anisotropic and unhomogeneous effects that may be present, only the material in the rim of the pancake is used for the manufacture of the specimens. The pancake is divided into twelve sections with eight specimen blanks per section. The in-plane view of one quarter of the pancake shown in Figure 3 defines the section geometry. The cross-sectional view of a typical section giving the specimen blank location is shown in Figure 4.

TABLE 1. COMPOSITION BY WEIGHT OF WROUGHT RENÉ 95.

	Weight % Alloy	
Alloying Element	Nominal	Range
Carbon	0.15	0.13 - 0.17
Chromium	14.0	13.0 - 15.0
Cobalt	8.0	7.0 - 9.0
Molybdenum	3.5	3.3 - 3.7
Columbium	3.5	3.3 - 3.7
Zirconium	0.05	0.03 - 0.07
Titanium	2.5	2.3 - 2.7
Aluminum	3.5	3.3 - 3.7
Boron	0.01	0.006- 0.015
Tungsten	3.5	3.3 - 3.7
Nickel	Remainder	Remainder

FIGURE 1. FORGED RENÉ 95 PANCAKE APPROXIMATELY 15 INCHES IN DIAMETER AND 1.75 INCHES THICK

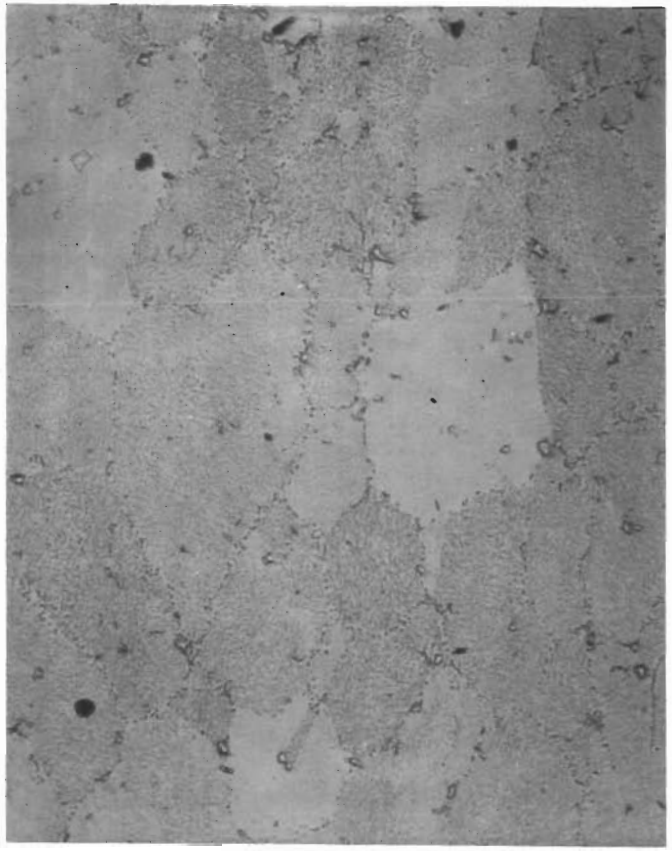

100X

(a)

100X

(b)

FIGURE 2. OPTICAL MICROGRAPHS OF RENÉ 95 IN A RADIAL PLANE: (a) NEAR THE RIM OF THE PANCAKE AND (b) ABOUT 2 CM (0.8 IN) FROM THE RIM.

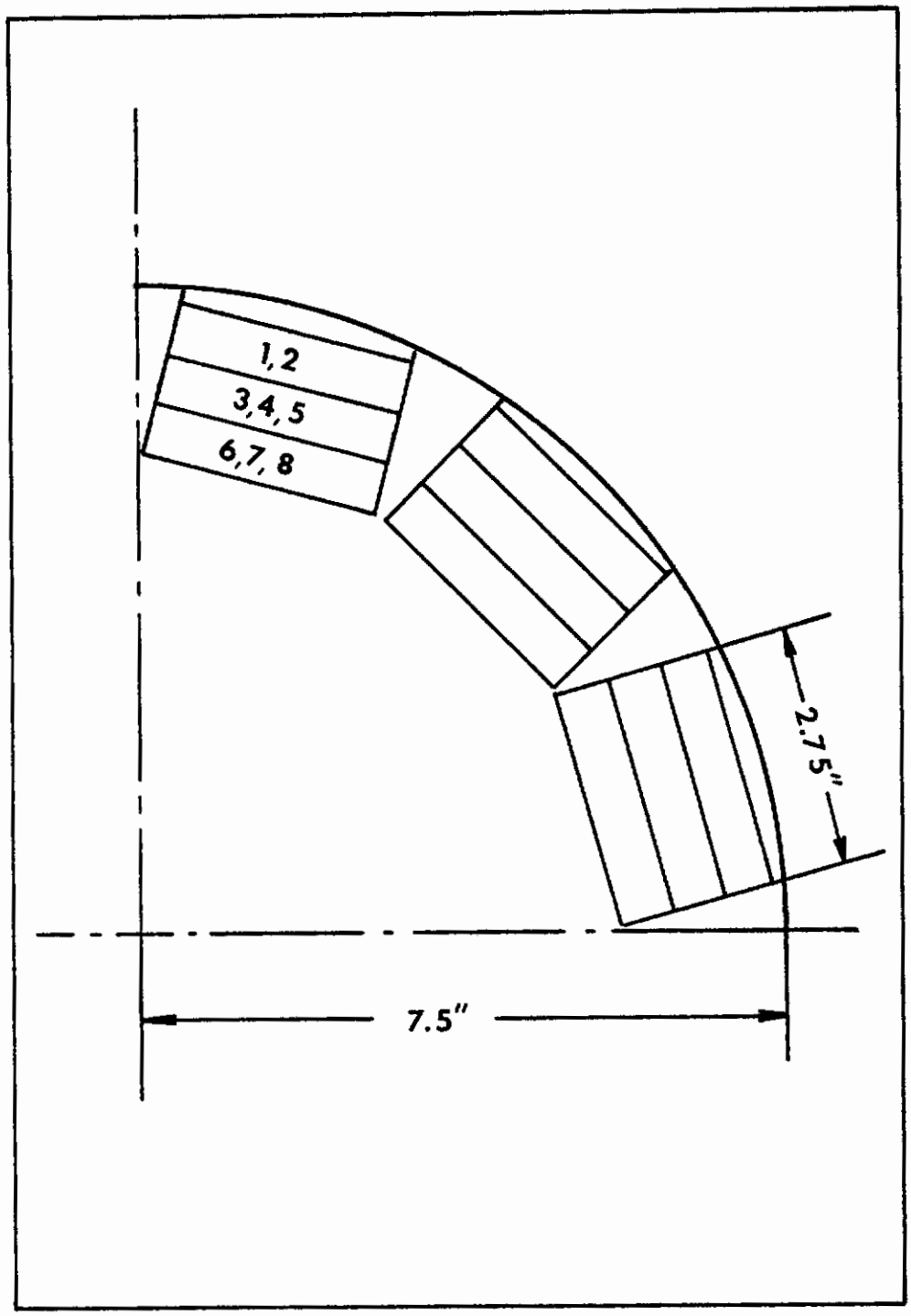

FIGURE 3. DIVISION OF THE RENÉ 95 PANCAKE INTO TWELVE SECTIONS WITH EIGHT SPECIMEN BLANKS IN EACH SECTION (ONE QUARTER OF PANCAKE SHOWN)

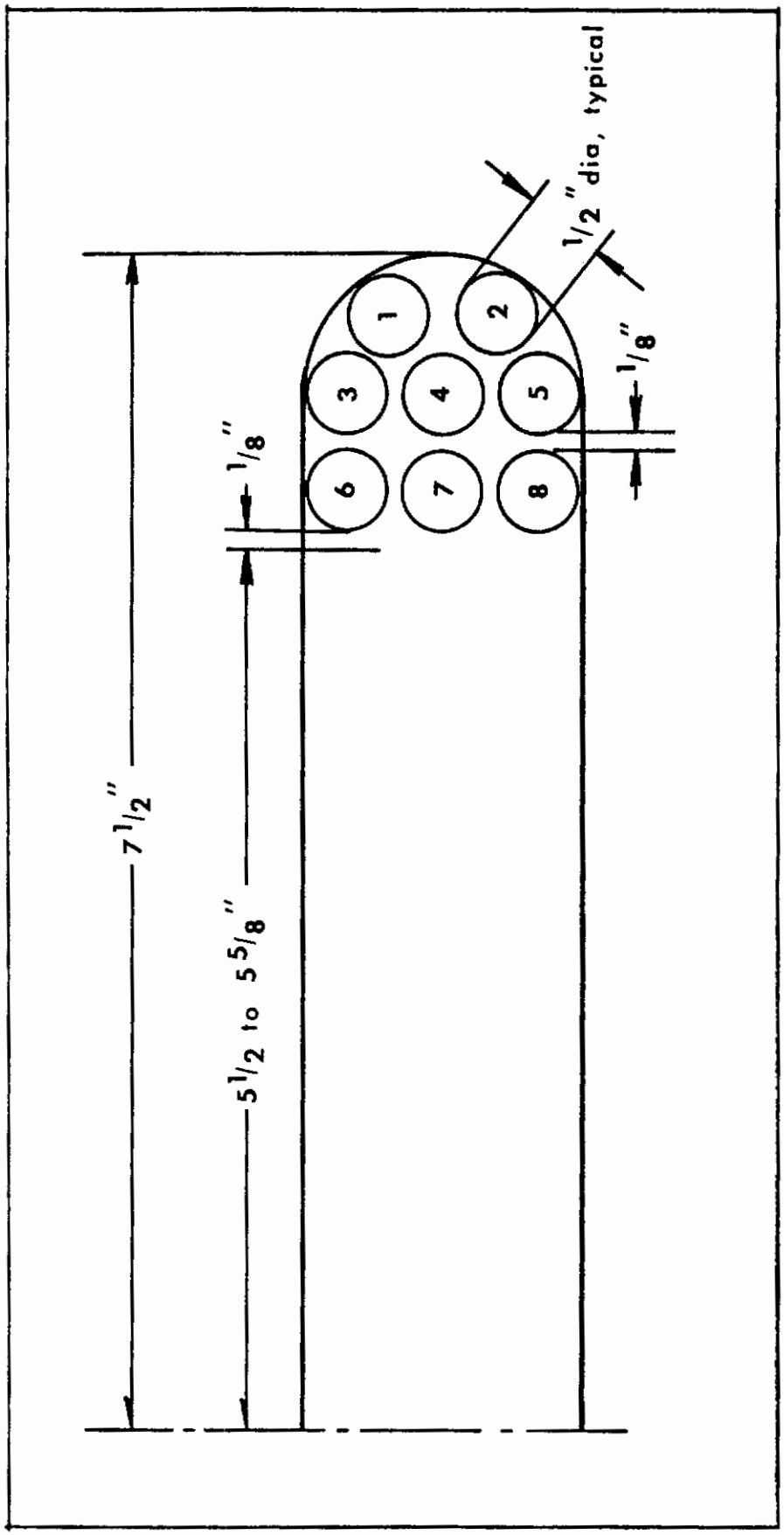

FIGURE 4 . LOCATION OF SPECIMEN BLANKS IN THE CROSS SECTION OF A RENÉ 95 PANCAKE

SECTION III
THE TESTING PROCEDURE

The experimental program described earlier generally requires specimens with more than one geometry. To help eliminate inconsistencies in data, the same specimen geometry was used for all tests. This resulted in picking the geometry shown in Figure 5 which is capable of providing reliable results in one dimensional tension and compression experiments for axial extensometry. The incompatability between the size of the specimen blanks and the specimen geometry was eliminated by inertia welding Inconel 718 cylinders onto the René 95 specimen blanks. Previous experience with this technique indicated that the inertia welding would not alter the René 95 microstructure in the test section of the specimen. The two material specimen structures were machined to the final geometry shown in Figure 5.

All experiments were performed in one testing machine at Mar-Test, Inc., Cincinnati, Ohio. The machine was custom made by Mar-Test and is a high performance closed-loop hydraulic system designed especially for high temperature, low cycle fatigue type of testing. The system employed an induction heater and water cooled grips. The extensometer, also developed by Mar-Test, was of axial design with long quartz rods that was attached directly to the specimen and set to a gage length of 0.500 inches. A typical set-up of a specimen in the machine is shown in Figure 6. Considering the reliability and outstanding control features of a machine designed for the low cycle fatigue tests, it was recognized that these features offer above average capabilities for creep and short time tensile and compressive testing as well. Special attention was given to the alignment of a specimen to minimize the eccentricity of the load and, to obtaining a uniform temperature profile in the test section.

The machine was run under either load or strain control as required by each particular experiment. The total strain, inelastic strain, load and temperature histories were recorded. The data generally was reduced using engineering stress and strain since the total strain range of interest did not exceed two percent.

A reference record of all tests run in this program is shown in Table 2. Each blank is marked with a sequence of two numbers, M-N. The first number, M, is the pancake section numbered clockwise from an arbitary starting point. The second number, N, specifies the location of the specimen blank in the cross section of the pancake. (Specimens were not manufactured from section 12.)

The letter code used for each specimen relates to the type of test and the number is the stress (KSI), strain (%), or strain rate (%/min) at which the test was run. The test matrix can be used with the experimental results to estimate the extent of anisotropy and homogeneity in the pancake.

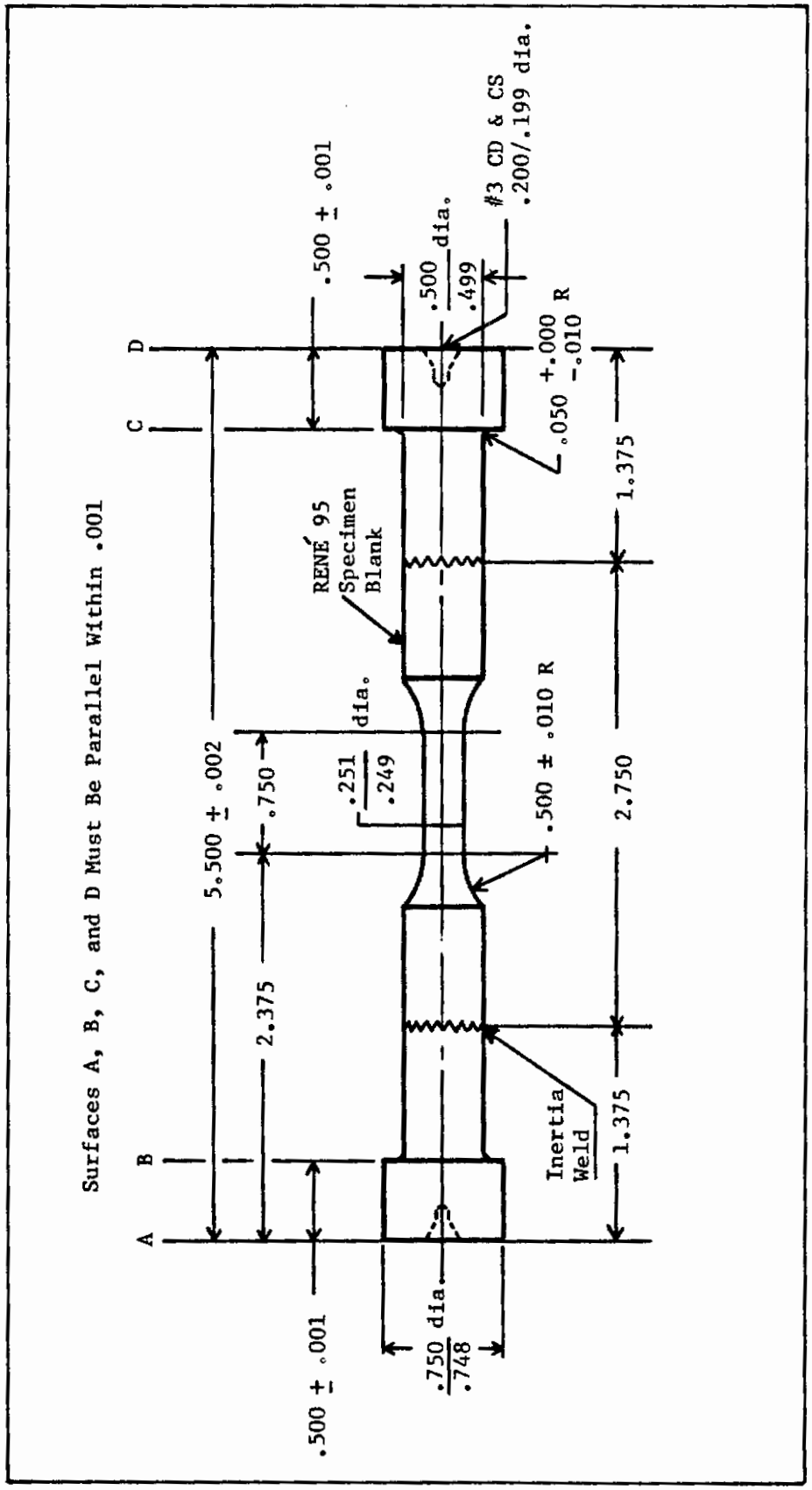

FIGURE 5 . GEOMETRY OF A SPECIMEN AFTER INERTIA WELDING

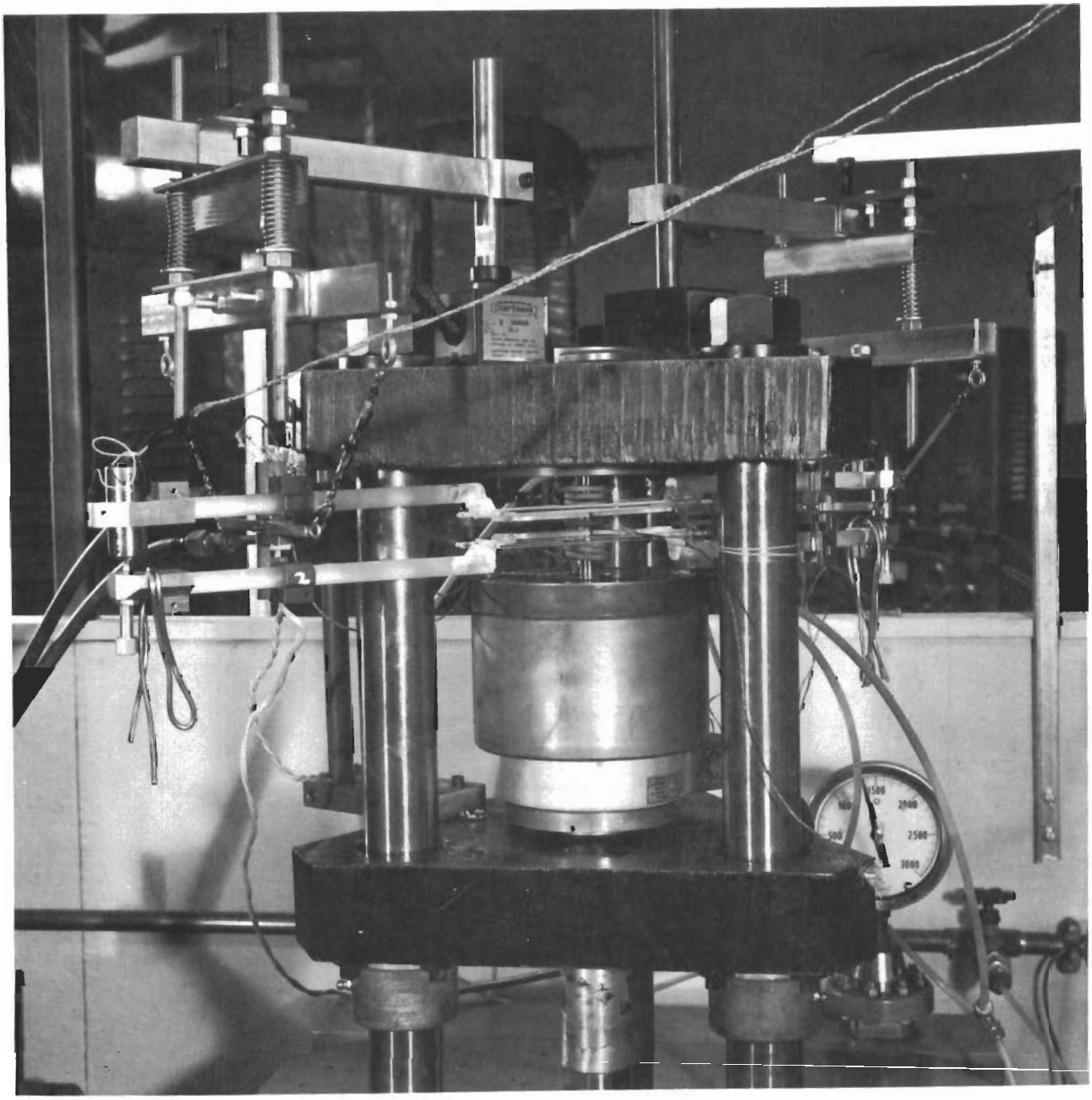

FIGURE 6. TESTING MACHINE AND SPECIMEN SET-UP SHOWN WITH TWO EXTENSOMETERS AS USED FOR COMPRESSIVE CREEP TESTS (GENERAL VIEW).

TABLE 2. MAP SHOWING POSITION OF SPECIMEN BLANK IN PANCAKE; Section number, M, and location, N, in section.

M \ N	1	2	3	4	5	6	7	8
1	TSS 50%/M	CSS -50.0%/M	TSS 0.05%/M	CSS -0.05%/M	TC 150 KSI	TC 167 KSI	TC 175 KSI	TC 158 KSI
2	TSS 10^{-3}%/M	TSS 60 KSI/M	LCF 164 KSI	CC 168 KSI	TC 168 KSI	LCF 134 KSI	MSC	TC,R 140 KSI
3		TSS 0.6 KSI/M	LCF 140 KSI	CC 147 KSI	TC 131 KSI	LCF 158 KSI	CC,R 150 KSI	TC,R 150 KSI
4	TSS 5%/MIN	TSS 0.05%/M	LCF 175 KSI	MSC	MSC		MSC	CC & LCF
5		LCF 78 KSI	LCF 168 KSI	MSC	TSS 6000 $\frac{KSI}{MIN}$	LCF 168 KSI	MSC	SR + 1.0%
6	TSS 5.0%/M	LCF 152 KSI		CC 160 KSI			MSC & Temper.	
7								
8				MSC				
9				CC 170 KSI				
10				CC 167 KSI				
11								

Notation:

TC = Tensile Creep at Constant Stress
CC = Compressive Creep at Constant Stress
MSC = Multiple Step Creep, Tension and Compression
TSS = Tensile Stress-Strain
CSS = Compressive Stress-Strain
LCF = Low Cycle Fatigue
SR = Stress Relaxation
R = Strain Recovery

SECTION IV
STRESS STRAIN RESPONSE

René 95 was evaluated to determine the stress response to a constant strain rate loading in tension and compression. The stress-strain curves for tensile constant strain rate tests at 50.0, 5.0, 0.05 and 0.001 percent per minute are shown in Figure 7. It can be seen that the response is ordered except at the highest strain rates; i.e. 5%/min and 50%/min. In this case, the stress strain curves are nearly identical, however the 5%/min test failed at 13.3% strain whereas the 50%/min test failed at 9.6% strain. Notice that all response curves appear to saturate at a constant stress (ultimate stress) and then drop off to a slightly lower stress prior to failure. This suggests a hardening mechanism in the material that saturates and remains nearly constant to failure; that is, the resistance to plastic flow is approximately constant at large values of strain.

Since these tests were run to failure, it is meaningful to replot the data as a function of "true" stress, $\sigma(1+\varepsilon)$, and "true" strain $\ln(1+\varepsilon)$, to estimate the real material response separate from the change in geometry of the test specimen. These response curves are shown in Figure 7a. Several important changes appear in the response curves. First the ultimate stress for tests 1, 2 and 3 are significantly higher. Second, in these curves, the ultimate stress remains essentially constant to failure. Thus, the drop off in ultimate stress shown in Figure 7 is geometric; i.e., as the cross sectional area of the specimen is reduced during a test, the load must be reduced to maintain a constant stress which produces the (imposed) constant strain rate. This further substantiates the stabilization of the material hardening mechanism. Third, the 50%/min test, Curve 1, does not appear to have saturated at a constant ultimate stress. Thus, there may be a unique relationship between strain rate and ultimate (true) stress.

For later use in life prediction, tensile tests were also conducted under constant load rate control corresponding to engineering stress rates of 41,400.0, 414.0, and 4.14 MPa per minute (6000, 60 and 0.6 KSI per minute) as shown in Figure 8. It is interesting to compare the stress-strain behavior shown in Figure 7, to the response shown in Figure 8. The curves taken under constant stress rate and constant strain rate exhibit different characteristics. The strain to failure is much less under stress control than under strain control and the stress rate control response does not saturate to a constant ultimate stress (as expected). Further, the stress-strain response curves are ordered with stress rate and do not suggest a saturation at higher stress rates; however, the variation in stress level over four decades of stress rate is much less than over the same variation in strain rate.

The stress-strain curves for compressive tests at constant strain rate are shown in Figure 9. These tests were terminated of about 2% total strain to avoid buckling and damage to the testing system. The initial response is ordered with the higher curve corresponding to the higher compressive strain rate. The magnitude of the shift in stress is slightly greater than the total variation due to strain rate in tension. However, it is expected that the strain rate effect in compression is also relatively small in the 0-2% strain range. It can also be observed from Figures 7 and 9 that the material is 5% to 10% stiffer in compression than in tension. If the tension and compression curves are replotted as functions of true stress (not shown) their appearance is essentially the same as shown except the difference between tensile and compressive behavior is reduced.

The combined results of the constant stress rate and strain rate tests indicate that the engineering stress-strain response of René 95 at 650°C (1200°F) is relatively insensitive to load rate or strain rate in the small (0

to 2%) strain range, except at very low rates. This conclusion is consistent with the results of Bernstein (Reference 7). In continuous cycling 20 CPM and 0.05 CPM tests, he showed there is essentially no difference in the fatigue loop dimensions (total strain range and total stress range). However, Bernstein did show that the fatigue life is sensitive to frequency (rate) even though the small strain stress-strain behavior is insensitive to rate.

A measure of the variation in the entire testing system, i.e., the machine, specimen, extensometer and recorders, can be estimated by the observed repeatability of the elastic modulus. As shown in Table 3, the elastic modulus for Renè 95 at 650°C (1200°F) is 174.8 MPa (25.2 KSI) ± 6%. Thus, it is reasonable to expect at least ± 6% variation in all other data.

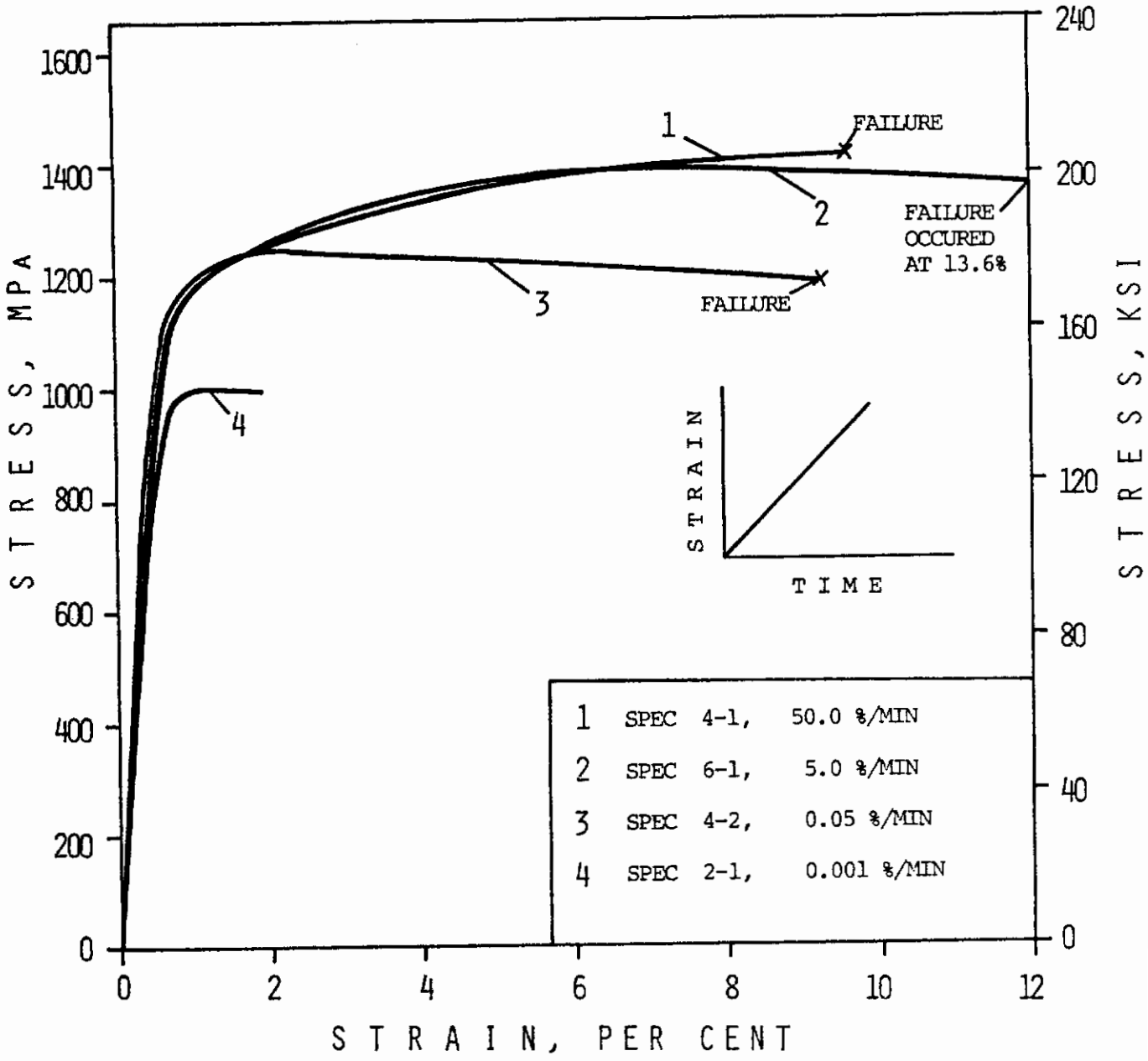

FIGURE 7. STRESS RESPONSE IN TENSION OF RENÉ 95 AT 650°C (1200°F) RUN UNDER CONSTANT STRAIN RATE CONTROL.

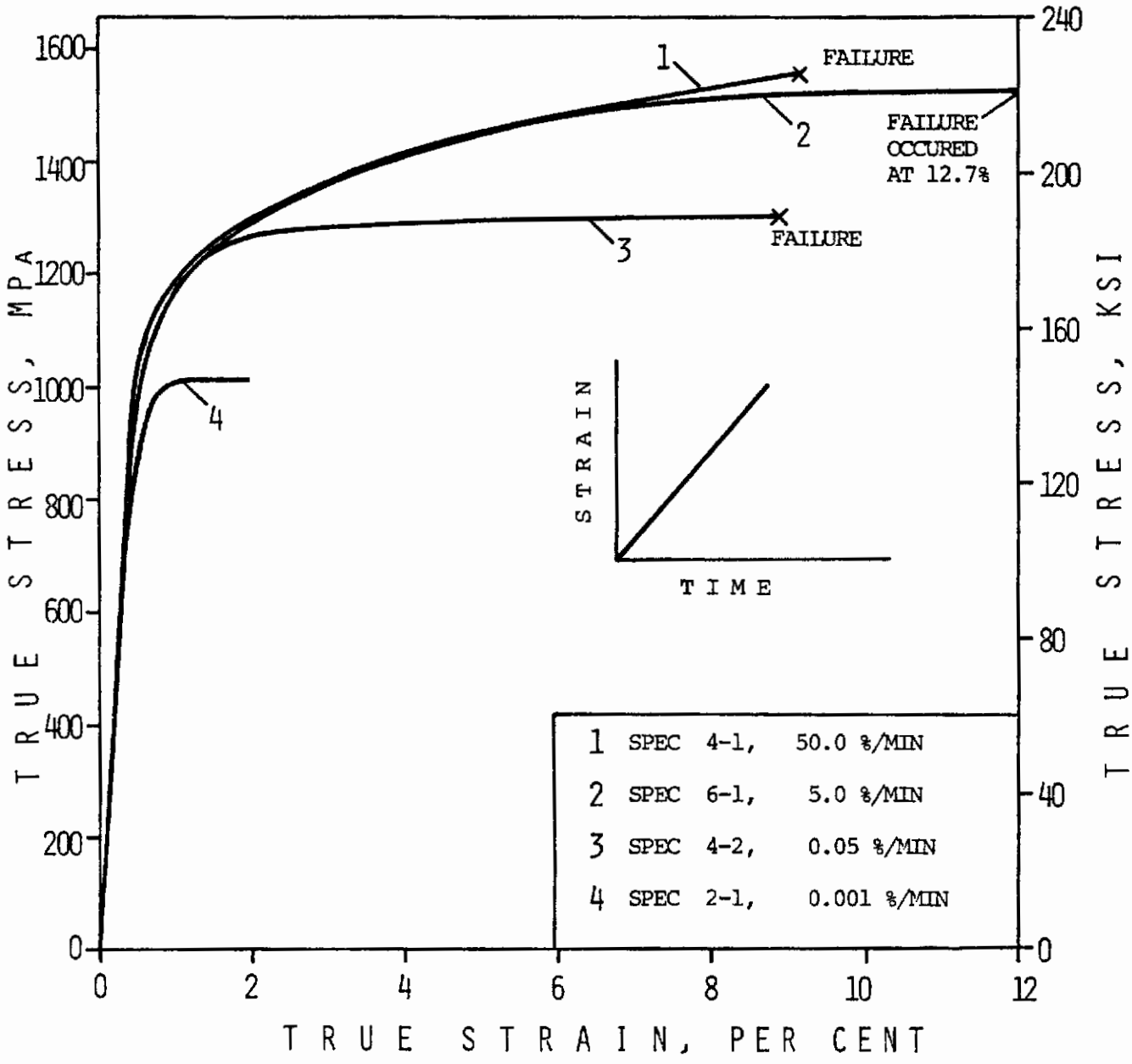

FIGURE 7a. TRUE STRESS VERSUS TRUE STRAIN DATA REPLOTTED FROM FIGURE 7.

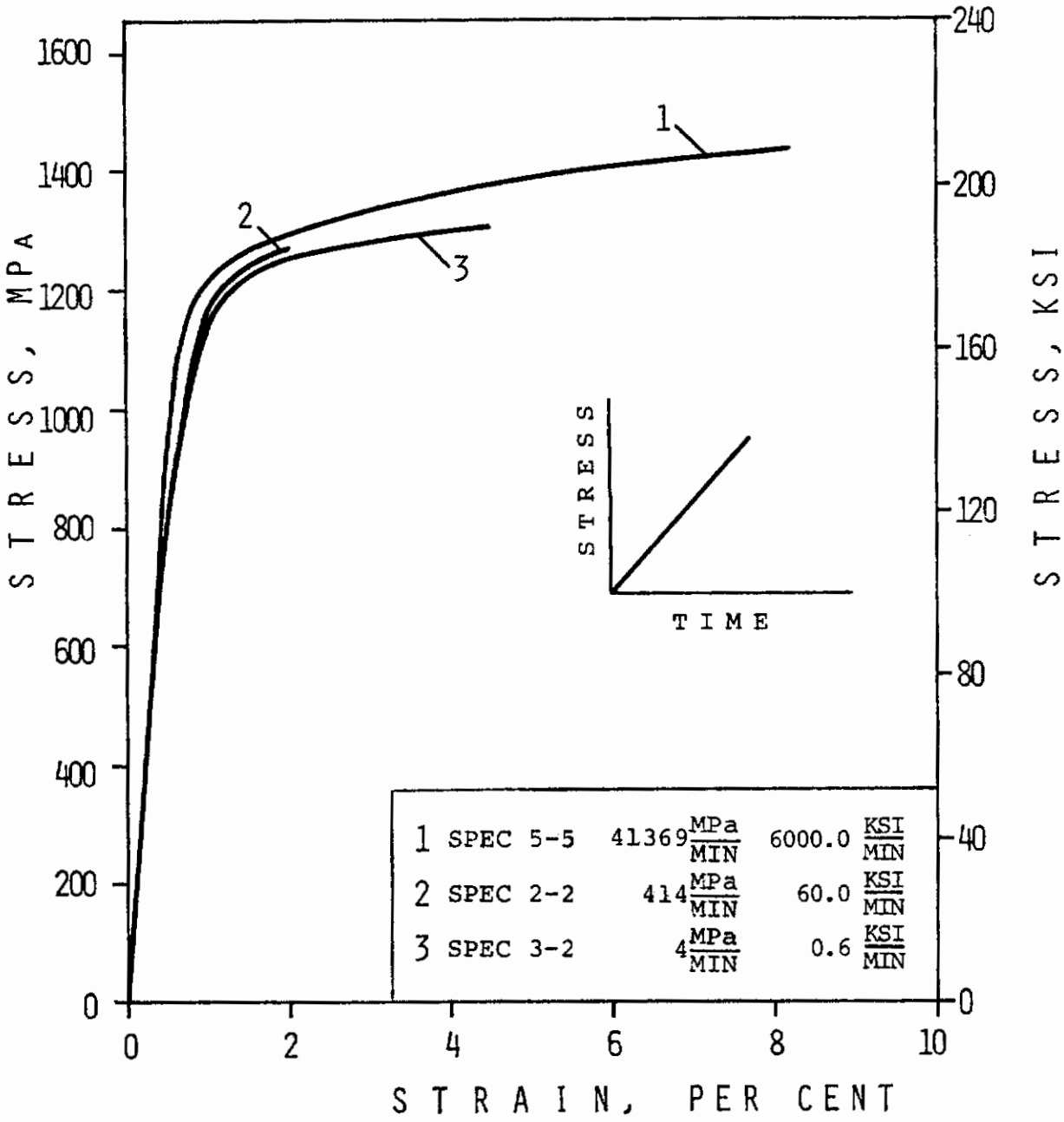

FIGURE 8. STRAIN RESPONSE AT CONSTANT STRESS RATE IN TENSION OF RENÉ 95 AT 650°C (1200°F).

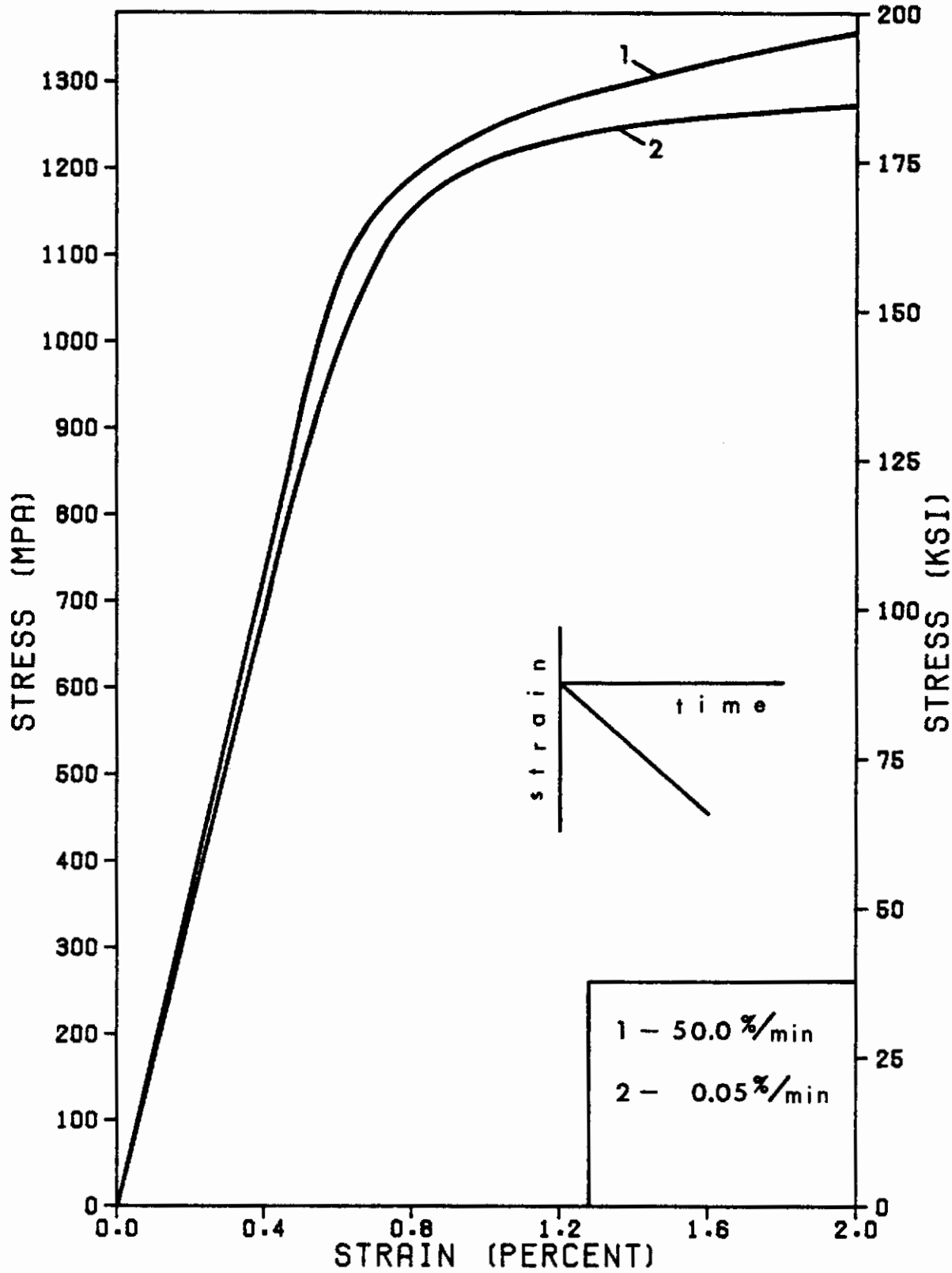

FIGURE 9 . STRESS RESPONSE IN COMPRESSION AT CONSTANT STRAIN RATE OF RENÉ 95 AT 650°C (1200°F)

TABLE 3. VARIATION OF ELASTIC MODULUS IN TENSION FOR RENÉ 95 AT 650°C (1200°F).

SPECIMEN NUMBER	ELASTIC MODULUS $x10^3$ MPa	$x10^3$ KSI
1-1	179.3	26.0
1-3	171.7	24.9
1-6	173.7	25.2
1-7	166.8	24.2
1-8	168.2	24.4
2-5	175.8	25.5
2-7	177.2	25.7
2-8	182.7	26.5
3-5	168.2	24.4
3-8	176.5	25.6
5-8	184.8	26.8
8-4	170.3	24.7
HIGH	184.8	26.8
LOW	166.8	24.2
MEAN	174.6	25.3

SECTION V
CREEP IN TENSION AND COMPRESSION

The tensile creep tests were run in the same machine using the same specimen design as for the stress-strain tests. In all tests, the load was applied in 1.5 to 10 seconds, which is at a rate corresponding to approximately 10 cycles per minute (CPM) in a fatigue test. Automatic loading was used for the higher stress tests. In the process of load application, the final load was not adjusted to the nominal value but left at the value obtained at the end of the automatic loading process. Eight nominal stress levels were used in tensile creep tests: 1207 MPa (175 KSI), 1156 MAa (167 KSI), 1089 MPa (158 KSI), 1034 MPa (150 KSI), 965 MPa (140 KSI), 903 MPa (131 KSI), 877 MPa (127 KSI) and 786 MPa (114 KSI).

A typical creep curve to failure is shown in Figure 10. The dominant features of response are the large tertiary creep region, the well defined linear or minimum creep region and the very small primary creep domain. In general, the objective of this work is to evaluate the material in the small strain region. Thus, tertiary creep is not included in the modeling and it is generally not included in this report. The small strain tensile creep curves are shown in Figures 11 and 12. The minimum creep rate is recorded in Table 4. Also shown in Table 4 is the time and strain at the onset of secondary and tertiary creep. A measure of the small amount of primary creep is denoted by "A"; the intersection of the slope of the curve in the secondary creep region with the strain axis (see Figure 11). At stresses below 1156 MPa (167 KSI) the inelastic primary strain is less than 0.4%. For convenience in later work, the three creep domains are shown in Figure 13 as a function of stress.

The distribution of the minimum creep rate with true stress and engineering stress is shown in Figure 14. Also plotted in Figure 14 is the ultimate stress from the stress-strain tests run using strain rate control (see Table 4).

The tests at 10^{-3}%/min., 5.0 x 10^{-2}%/min. and 5.0%/min. have well defined regions of constant stress that can be seen in Figures 7 and 7a. The test at 50%/min. is not included since a saturation ultimate stress may not have been reached. These data are included in Figure 14 since the condition of constant stress and constant strain rate appears to correspond to the minimum creep condition. Thus, the ultimate stress in a constant strain rate test can be identified as a creep stress.

These data explain the apparent rate independence of René 95 at the high strain rates. In Figure 14, it is clear that the slope of the stress-creep rate curve becomes steeper at increasing stress levels. Thus, increasing the strain rate above 5%/min. will not significantly change the ultimate stress in an engineering stress-strain curve. However, note that in higher strain rates tests the ultimate stress occurs at larger strains. If the minimum creep data is plotted as a function of true stress (not shown), it is found that much of the curvature is removed and the strain rate sensitivity does not appear to saturate at the higher true stress levels. This observation implies that the same deformation mechanism could be active at all levels of true stress considered.

In a recent report by Bodner (Reference 21), on the same material at the same temperature, he considers more than one deformation mechanism to be present over a similar range of creep tests. At the higher stress levels, he explains the saturation of strain rate dependence to arise from a change in creep mechanism. At this point, the question of the number of active mechanisms is to be open, and resolution does not appear possible with the assistance of a metallurgical study.

Compressive creep studies were attempted using one axial extensometer similar to the tensile creep tests; however, bending of the specimen produced

unreliable data. These experiments were repeated using two axial extensometers mounted diagonally across the specimen. The two extensometer creep measurements were averaged and results are shown in Figures 15 and 16, and also in Table 5. The data was discarded when the measurements diverged indicating buckling. The response also indicates a small primary creep region and relatively large secondary creep domain (tertiary creep was not included). The most significant observation is that the minimum creep rate in compression is about a factor of ten lower than in tension. This observation is important for modeling since creep in tension and compression cannot be considered to be the same.

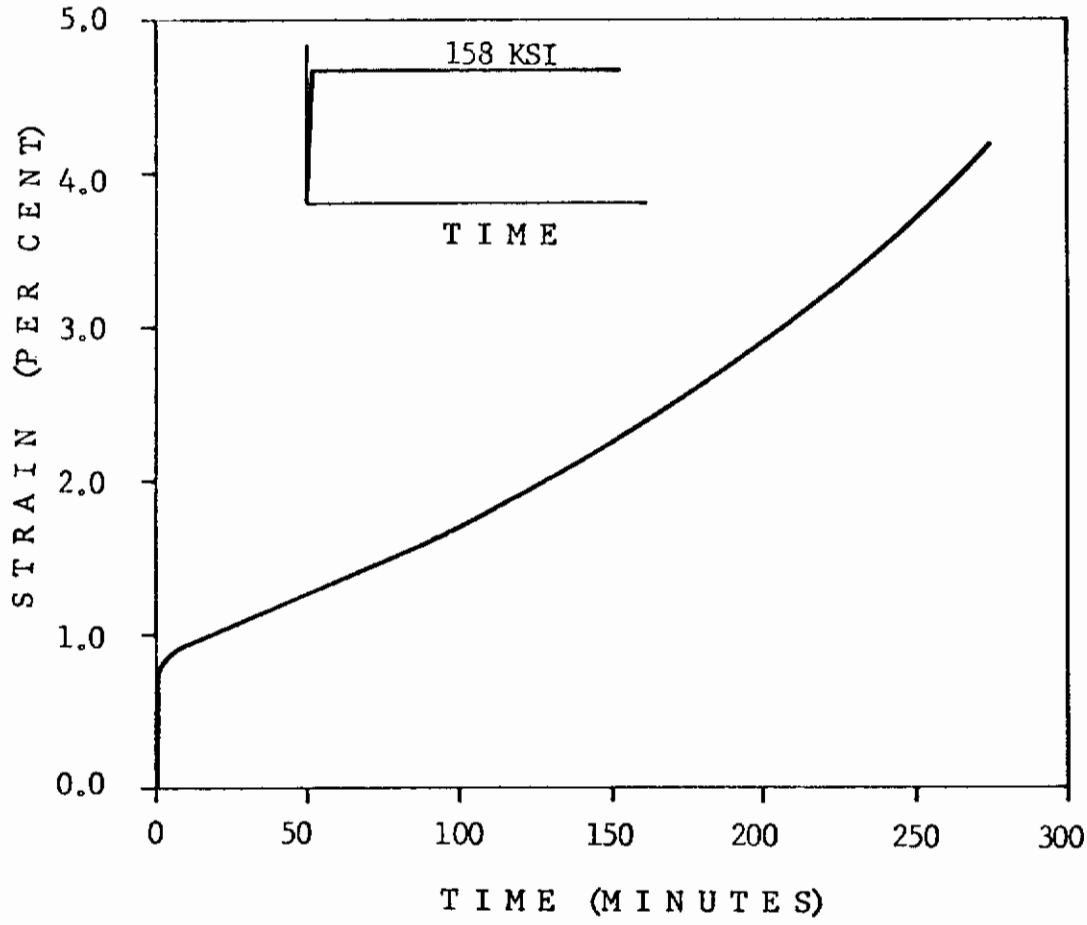

FIGURE 10. TYPICAL CREEP RESPONSE CURVE FOR RENÉ 95 AT 650°C (1200°F). THIS EXPERIMENT WAS RUN AT 1089.4 MPa (158 KSI). SPECIMEN 1-8.

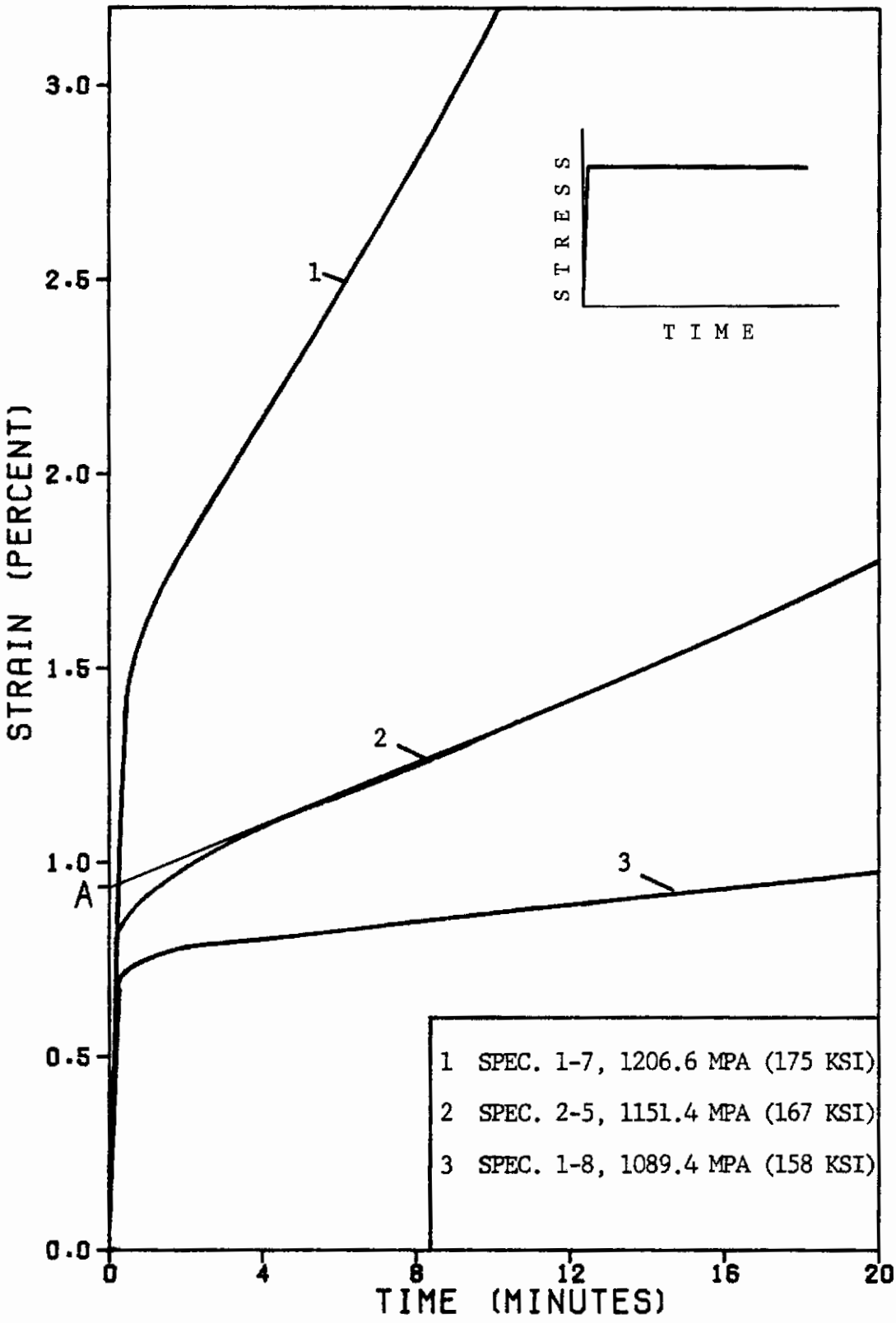

FIGURE 11. TENSILE CREEP RESPONSE AT THE HIGHER LEVELS OF STRESS OF RENÉ 95 AT 650°C. (1200°F.).

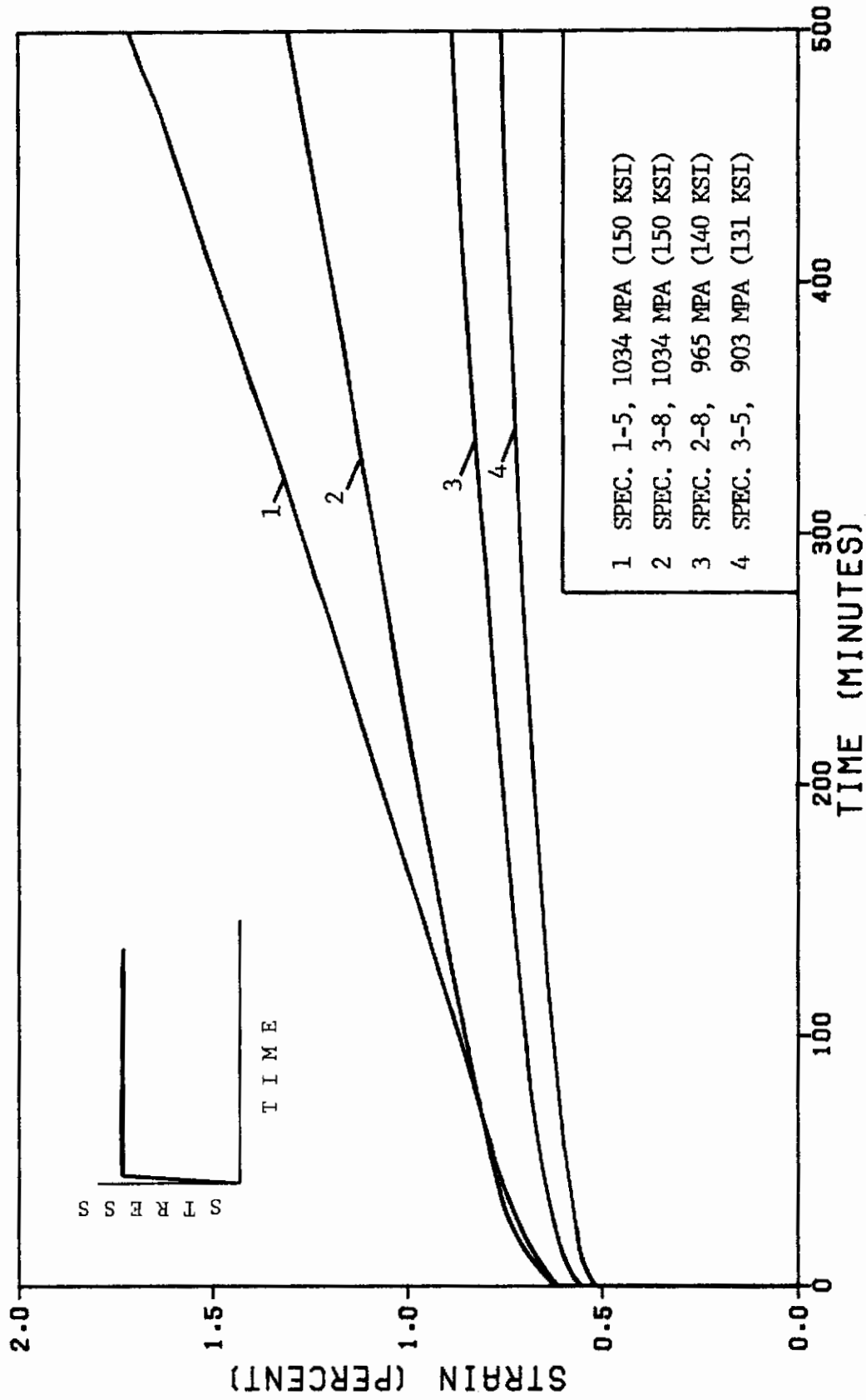

FIGURE 12. TENSILE CREEP RESPONSE AT THE LOWER STRESS LEVELS OF RENE 95 AT 650°C. (1200°F.).

STRESS MPa (KSI)	SPEC. NUMBER	A %	MIN CREEP RATE %/MIN.	TRUE STRESS DURING MIN CREEP MPa (KSI)	ONSET SECONDARY CREEP		ONSET TERTIARY CREEP	
					TIME MIN.	STRAIN %	TIME MIN.	STRAIN %
786.0 (114.0)	4-5	0.485	4.0×10^{-5}	786 (114)	250	0.490	‡	‡
877.0 (127.2)	2-7	0.610	3.21×10^{-4}	883 (128)	120	0.750	‡	‡
903.5 (131.0)	3-5	0.630	2.76×10^{-4}	912 (132)	210	0.730	2750	1.410
965.3 (140.0)	2-8	0.680	4.4×10^{-4}	975 (141)	775	0.760	1450	1.340
1034.3 (150.0)	3-5	0.750	1.15×10^{-3}	1047 (152)	60	0.810	750	1.60
1034.3 (150.0)	1-5	0.680	2.0×10^{-3}	1047 (152)	50	0.720	350	1.40
1089.4 (158.0)	1-8	0.780	9.1×10^{-3}	1103 (160)	4	0.780	100	1.70
1156.3 (167.7)	2-5	0.940	4.0×10^{-2}	1174 (170)	2	1.040	22	1.92
1206.6 (175.0)	1-7	1.490	1.63×10^{-1}	1234 (179)	1	1.680	9	2.95

‡ Tertiary creep range not obtained in these experiments.

Table 5. Summary of tensile creep response data for Rene 95 at 650°C (1200°F).

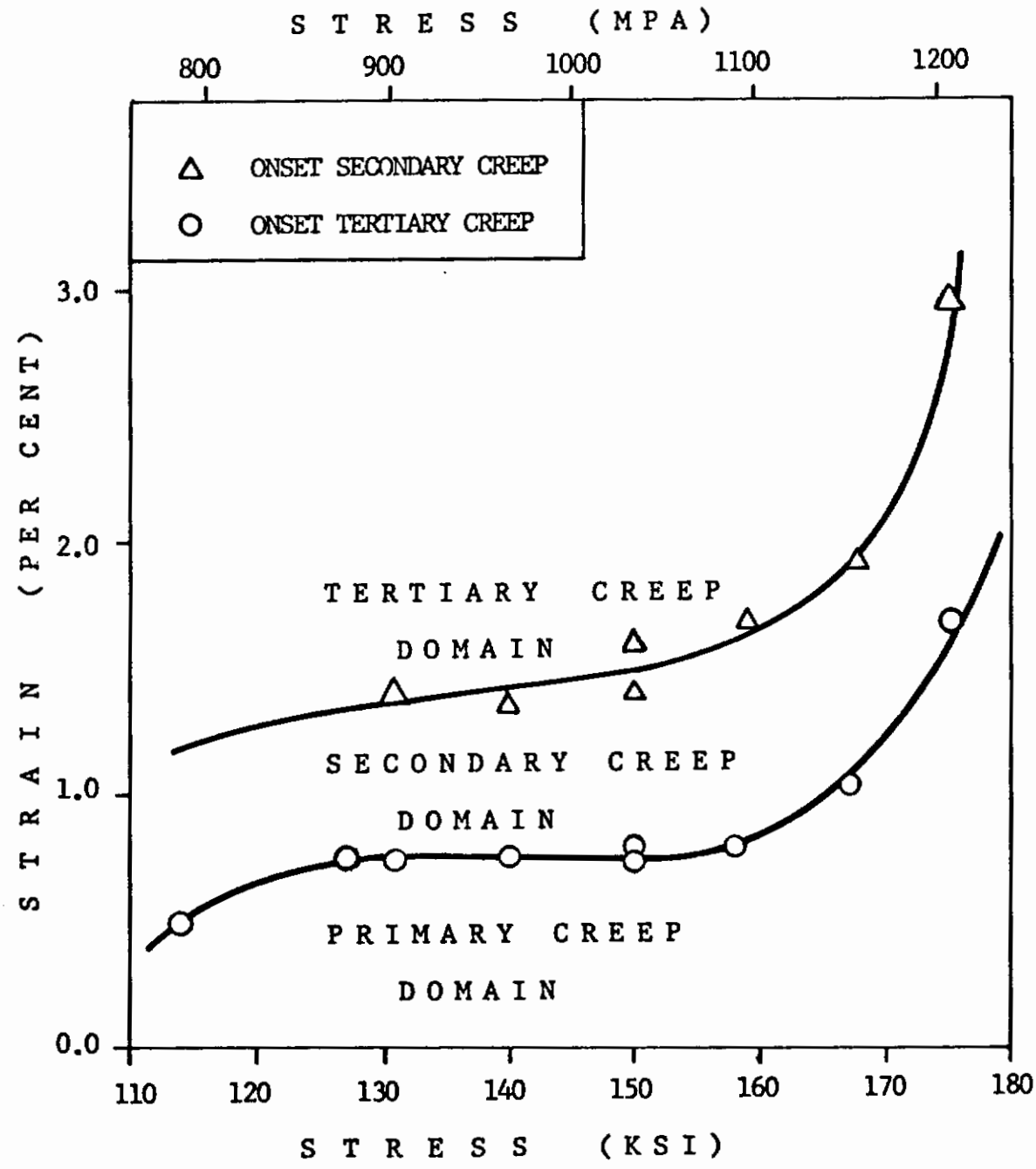

FIGURE 13. AN ESTIMATE OF THE THREE TENSILE CREEP RESPONSE DOMAINS FOR RENÉ 95 AT 650°C (1200°F).

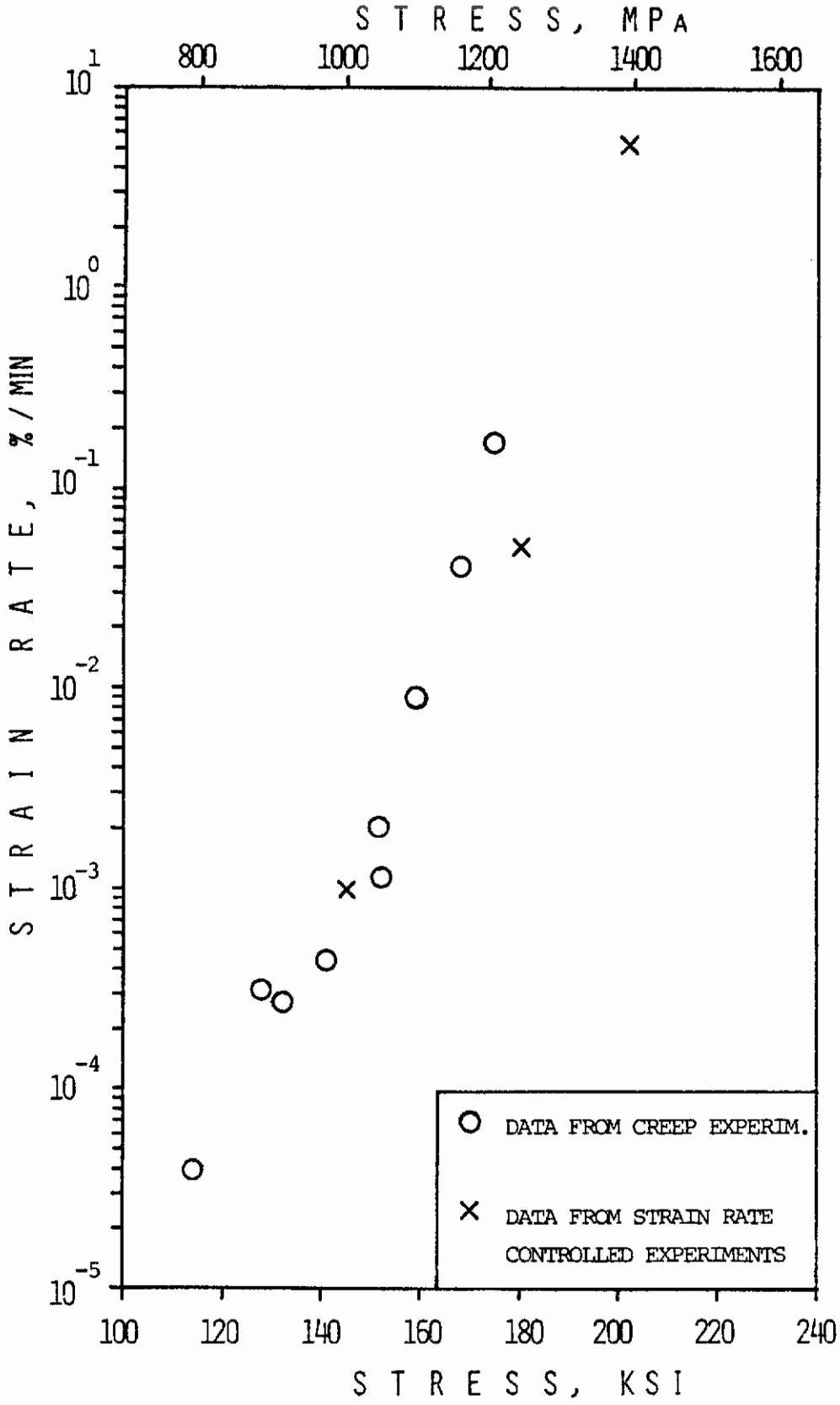

FIGURE 14. DISTRIBUTION OF MINIMUM CREEP RATE AS A FUNCTION OF STRESS FOR RENÉ 95 AT 650°C (1200°F).

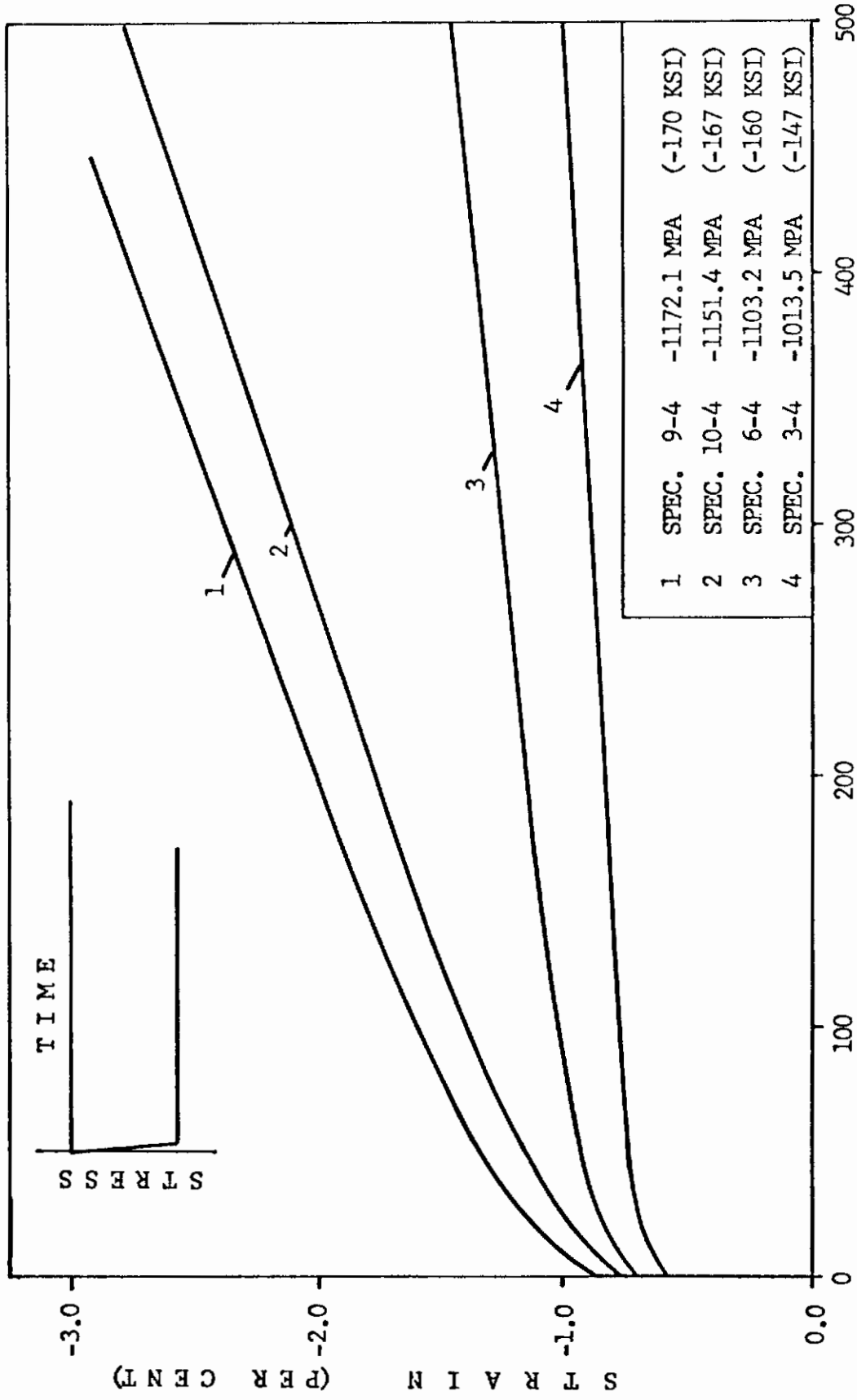

FIGURE 15. COMPRESSIVE CREEP RESPONSE AT FOUR STRESS LEVELS OF RENÉ 95 AT 650°C (1200°F)

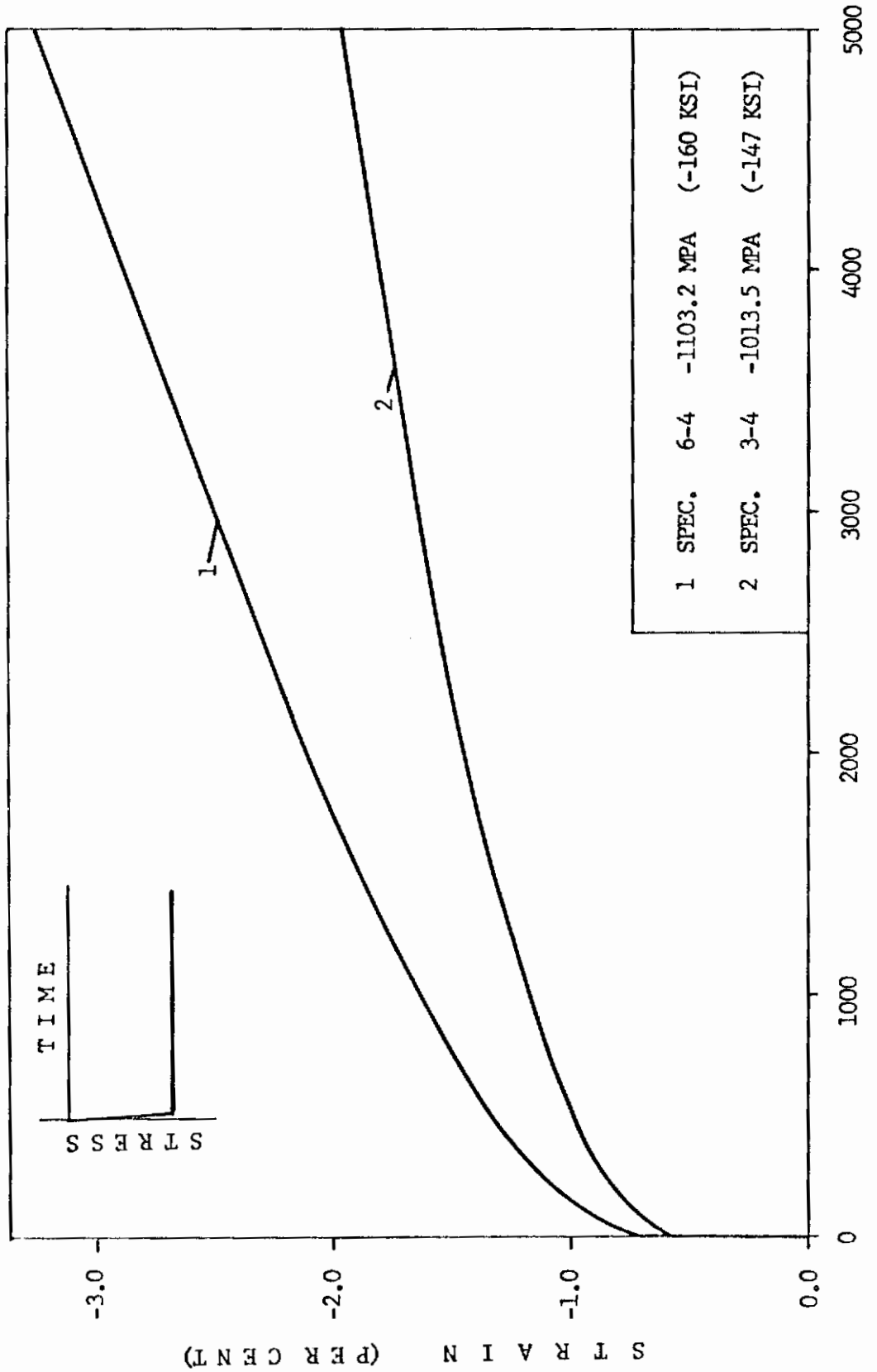

FIGURE 16. COMPRESSIVE CREEP RESPONSE AT LOWER STRESS LEVELS OF RENÉ 95 AT 650°C (1200°F)

TABLE 5. SUMMARY OF COMPRESSIVE CREEP RESPONSE DATA FOR RENÉ 95 AT 650°C (1200°F).

Stress MPa (KSI)	Spec. Number	A %	Min. Creep Rate %/Min.	Onset Secondary Creep	
				Time Min.	Strain %
-1013.5 (-147)	3-4	-0.69	-1.6×10^{-4}	250	2.20
-1103.2 (-160)	6-4	-0.97	-9.6×10^{-4}	175	1.67
-1151.4 (-167)	10-4	-1.10	-3.3×10^{-3}	150	1.10
-1172.1 (-170)	9-4	-1.28	-3.6×10^{-3}	75	0.75

SECTION VI
MULTI-STEP TENSILE CREEP HISTORIES

One of the objectives of this program is to develop an understanding of cyclic fatigue with intervals of hold time. However, these results are generally very complicated to use in the development of constitutive theories because the phenomena controlling the deformation cannot be isolated. A much simpler experiment is to investigate tensile creep response with step changes in stress at different times in the history. A second level of investigation to include reverse inelastic flow is planned.

The main issue is to learn to what extent the minimum creep rate is dependent on the load sequence history. Five experiments in this category are outlined in Table 6. Specimens 5-7 and 6-7 were loaded and unloaded through the same stress levels, as shown. Typical of all results, the creep response for specimens 5-7, 6-7 and 2-7 are shown in Figures 17, 19, and 21, respectively; and, the corresponding stress-strain response is shown in Figures 18, 20, and 22, respectively.

Let us begin the analysis of the response by observing that the time duration of steps 1 and 5, and, 2 and 4 for specimen 5-7 (Figure 17) are 50 minutes and 15 minutes, respectively. If the creep rate, for example, is the same constant value during stress steps 1 and 5, the same amount of strain would be accumulated during the two 50 minute intervals. Using Figure 18, it is obvious that the accumulated strain during steps 1 and 5, and, 2 and 4 are not equal, respectively. The differences are relatively small considering the scatter in the minimum creep rate shown in Figure 14. Further, by comparing the creep data from specimen 5-7 with the secondary creep region shown in Figure 13, it can be seen that the material is in a primary creep domain during step 1 and a transition to tertiary creep occurs during steps 4 and 5.

Thus, it is not expected that the accumulated strain during intervals of equal stress and time would be exactly equal.

This same general pattern can be observed in all five step creep tests recorded in Table 6. The creep rate is in transition from primary to secondary to tertrary during the experiment. However, the accumulated strains during equal time and stress intervals were approximately the same except for the initial loading. This follows since remaining creep rates were relatively close to the minimum creep rate.

To further investigate the effect of step stress changes on the response, the average strain rate (linear segments of Figures 17, 19 and 21) during each interval was plotted as a function of stress for each test as shown in Figure 23. The most interesting feature of Figure 23 is that all data from each test are approximately linear, and that the lines from all five tests are very close to parallel. The order of the stress sequence does not appear to change the strain rate response. Thus, we conclude if the strain rate is near or in the secondary creep domain, the response is independent of ordering of the step stress history.

The minimum creep rate data also falls within the envelope of response to the step stress history tests. The data appear to cluster around the tests from specimens 2-7, 6-7, and 8-4. Thus, we conclude that these tests represent a reasonable estimate of the nominal stress-strain rate response of René 95 at 1200°F. Further, the spread of the data is a measure of the extent of variation in response from specimen to specimen. These variations are typical of the lack of repeatability for high temperature material study.

The effect of changes in temperature was also investigated. Following the six-step creep test on specimen 4-5, the temperature was adjusted as shown in Table 7 to measure the effect of temperature on the minimun creep rate.

The stress was held constant at 1089.4 MPa (158 KSI) and the total strain did not exceed 2%. The material was beginning tertiary creep, however; micro-cracking and cracking is not expected to be present since the specimen was well below the average failure strain of 6% to 8%. Under these conditions the activation energy, λ, corresponding to relatively stable microstructure, can be calculated using the rate equation

$$\dot{\varepsilon} = A \exp(-\lambda/RT)$$

where A is a constant, T the absolute temperature and the ideal gas constant R = 1.98 cal/mole/°K. For René 95 in these conditions, λ = 112000 cal/mole.

TABLE 6. EFFECT OF STEP CHANGES IN TENSILE STRESS ON THE CREEP OF RENÉ 95 AT 650°C (1200°F).

SPEC. NO.	EVENT NO.	STRESS MPa (KSI)	DURATION MIN.	AVERAGE STRAIN RATE %/MIN.	FINAL STRAIN %
5-7	1	903 (131.0)	50	2.1×10^{-3}	0.722
	2	1034 (150.0)	15	1.1×10^{-2}	0.960
	3	1207 (175.0)	5	1.5×10^{-1}	1.880
	4	1034 (150.0)	15	1.6×10^{-2}	2.044
	5	903 (131.0)	50	2.3×10^{-3}	2.088
6-7	1	965 (140.0)	710	9.16×10^{-4}	1.360
	2	1089 (158.0)	40	7.0×10^{-3}	1.680
	3	1207 (175.0)	8	4.6×10^{-2}	2.100
	4	1089 (158.0)	31	1.0×10^{-2}	2.360
	5	965 (140.0)	200	1.4×10^{-3}	2.600
2-7	1	877 (127.2)	1300	3.21×10^{-4}	1.062
	2	1005 (145.7)	220	2.40×10^{-3}	1.416
	3	877 (127.2)	1300	3.37×10^{-4}	1.760
	4	763 (110.7)	1200	6.00×10^{-5}	1.778
	5	824 (119.5)	1300	1.33×10^{-4}	2.018
	6	731 (106.0)	1328	-	1.952
4-5	1	786 (114.0)	1393	4.0×10^{-5}	0.523
	2	903 (131.0)	1061	5.67×10^{-5}	0.674
	3	1034 (150.0)	69	7.50×10^{-4}	0.800
	4	786 (114.0)	1015	1.8×10^{-5}	0.706
	5	1034 (150.0)	135	1.05×10^{-3}	0.930
	6	1151 (167.0)	101	3.71×10^{-3}	1.393
8-4	1	1195 (173.3)	8	5.2×10^{-2}	1.928
	2	967 (140.2)	60	1.83×10^{-3}	1.948
	3	1087 (157.7)	51	6.5×10^{-3}	2.360

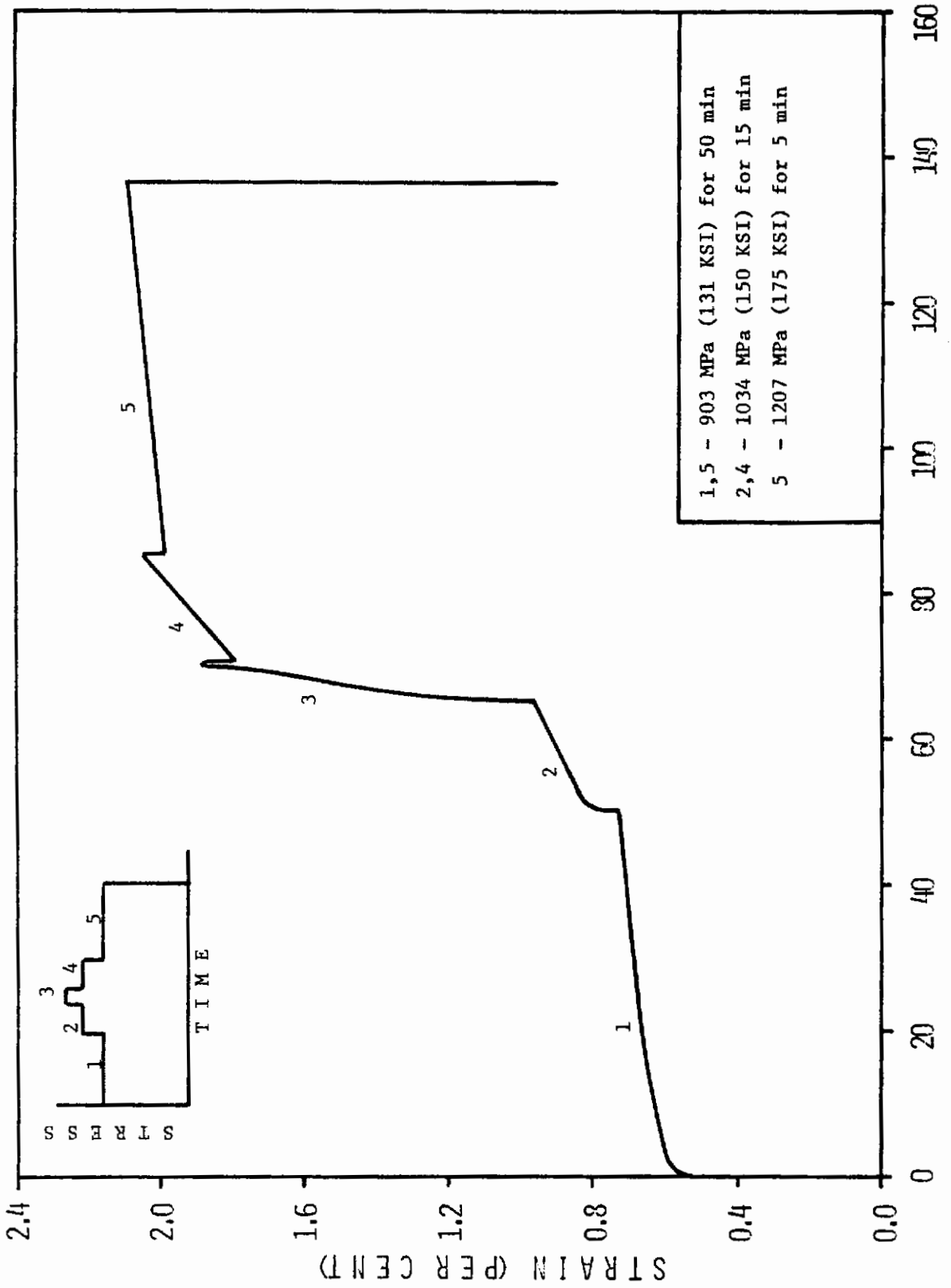

FIGURE 17. TENSILE CREEP RESPONSE OF SPECIMEN 5-7 DUE TO A FIVE STEP STRESS HISTORY OF RENÉ 95 AT 650°C (1200°F)

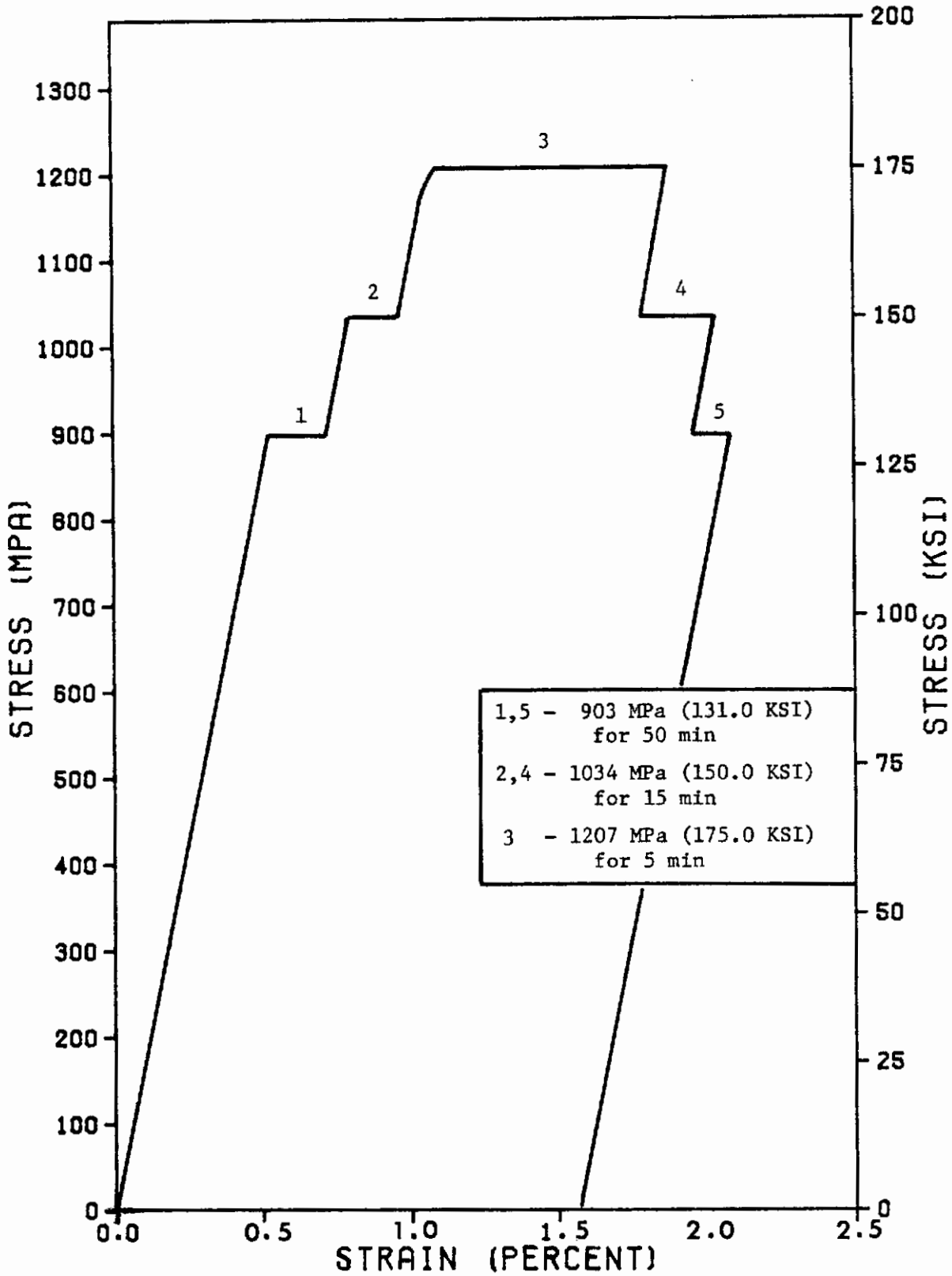

FIGURE 18 . STRESS-STRAIN RESPONSE OF SPECIMEN 5-7 DUE TO A FIVE STEP STRESS HISTORY OF RENÉ 95 AT 650°C (1200°F)

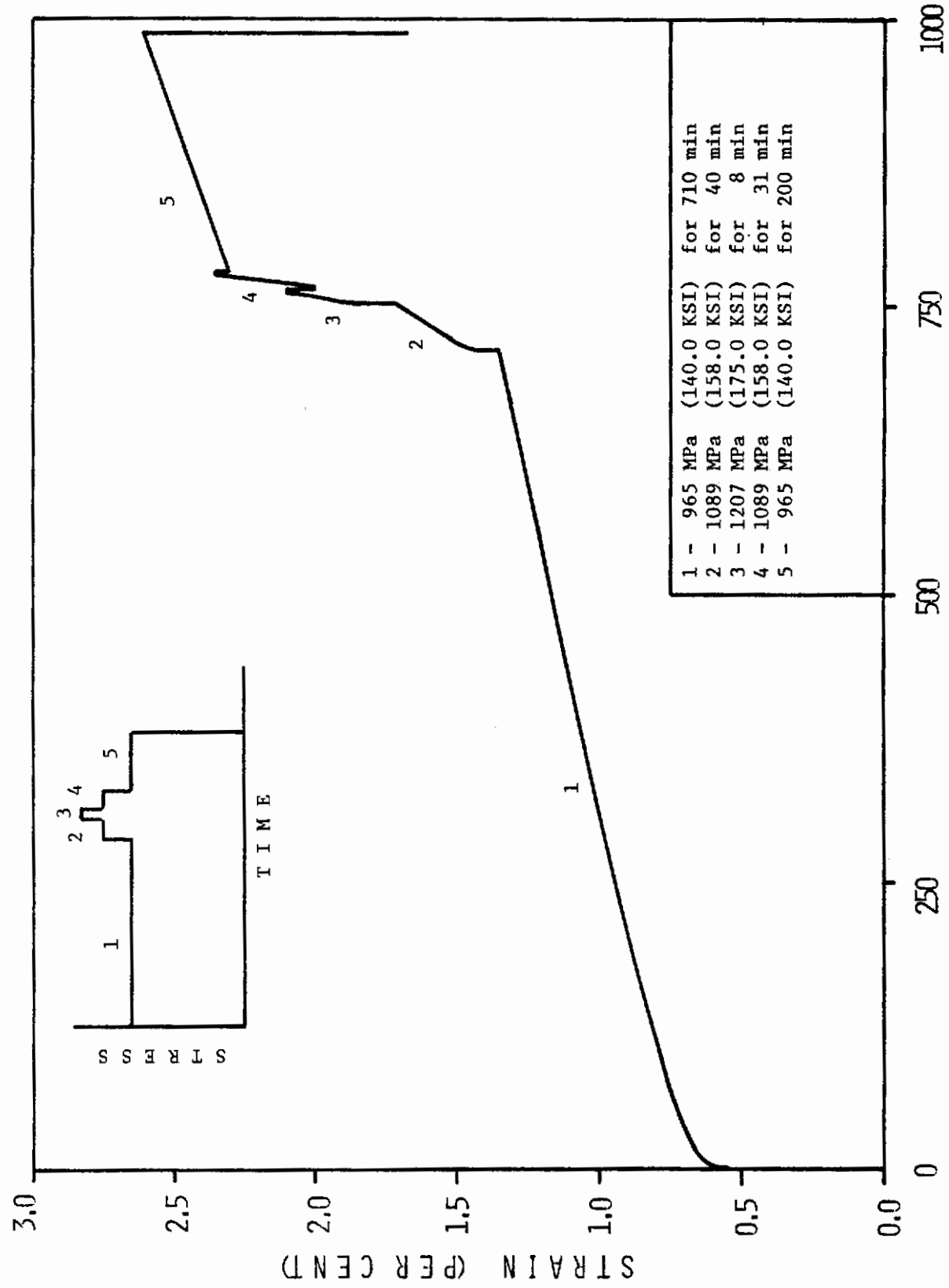

FIGURE 19. TENSILE CREEP RESPONSE OF SPECIMEN 6-7 DUE TO A FIVE STEP STRESS HISTORY OF RENÉ 95 AT 650°C (1200°F)

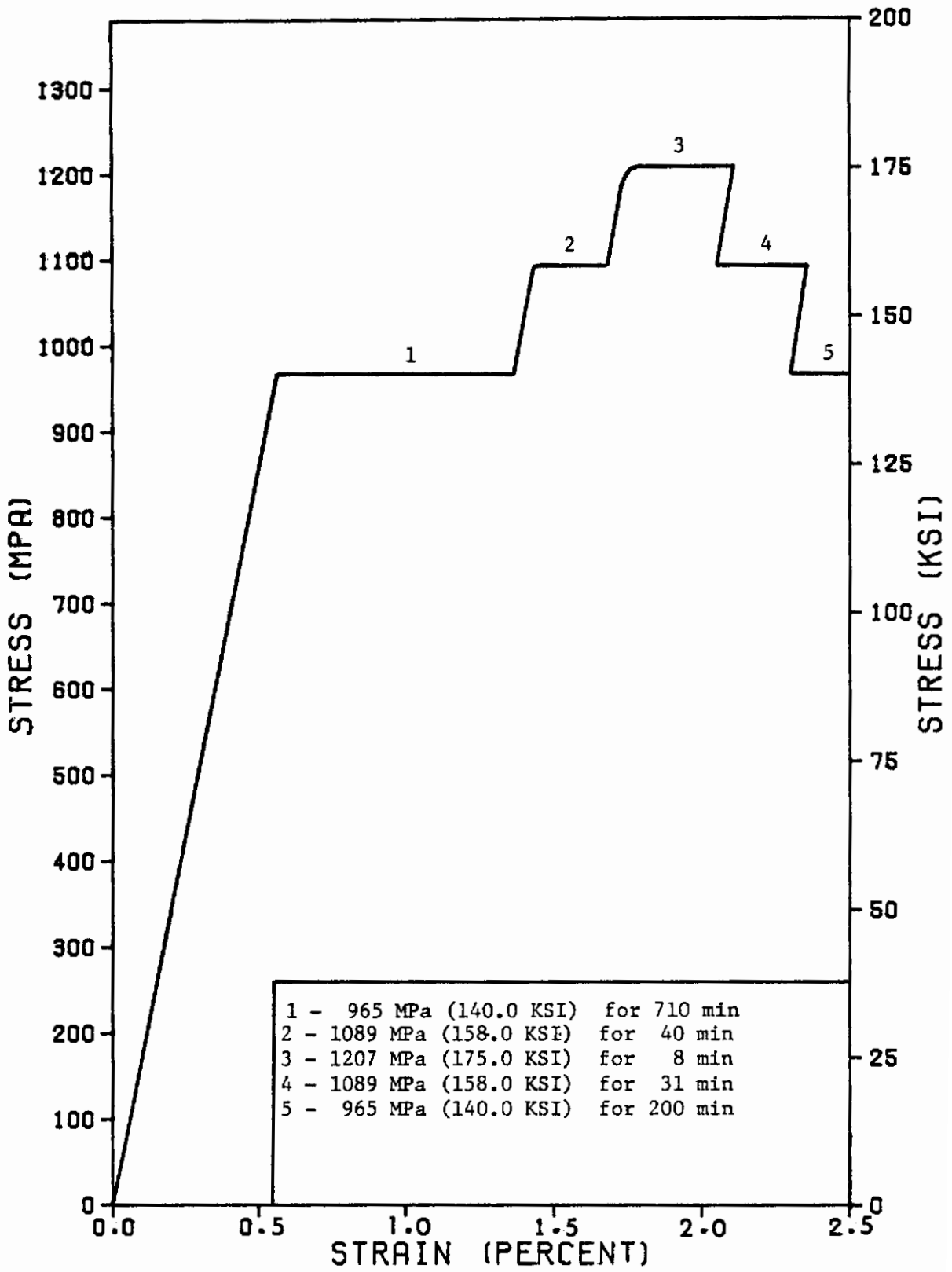

FIGURE 20. STRESS-STRAIN RESPONSE OF SPECIMEN 6-7 DUE TO A FIVE STEP STRESS HISTORY OF RENÉ 95 AT 650°C (1200°F)

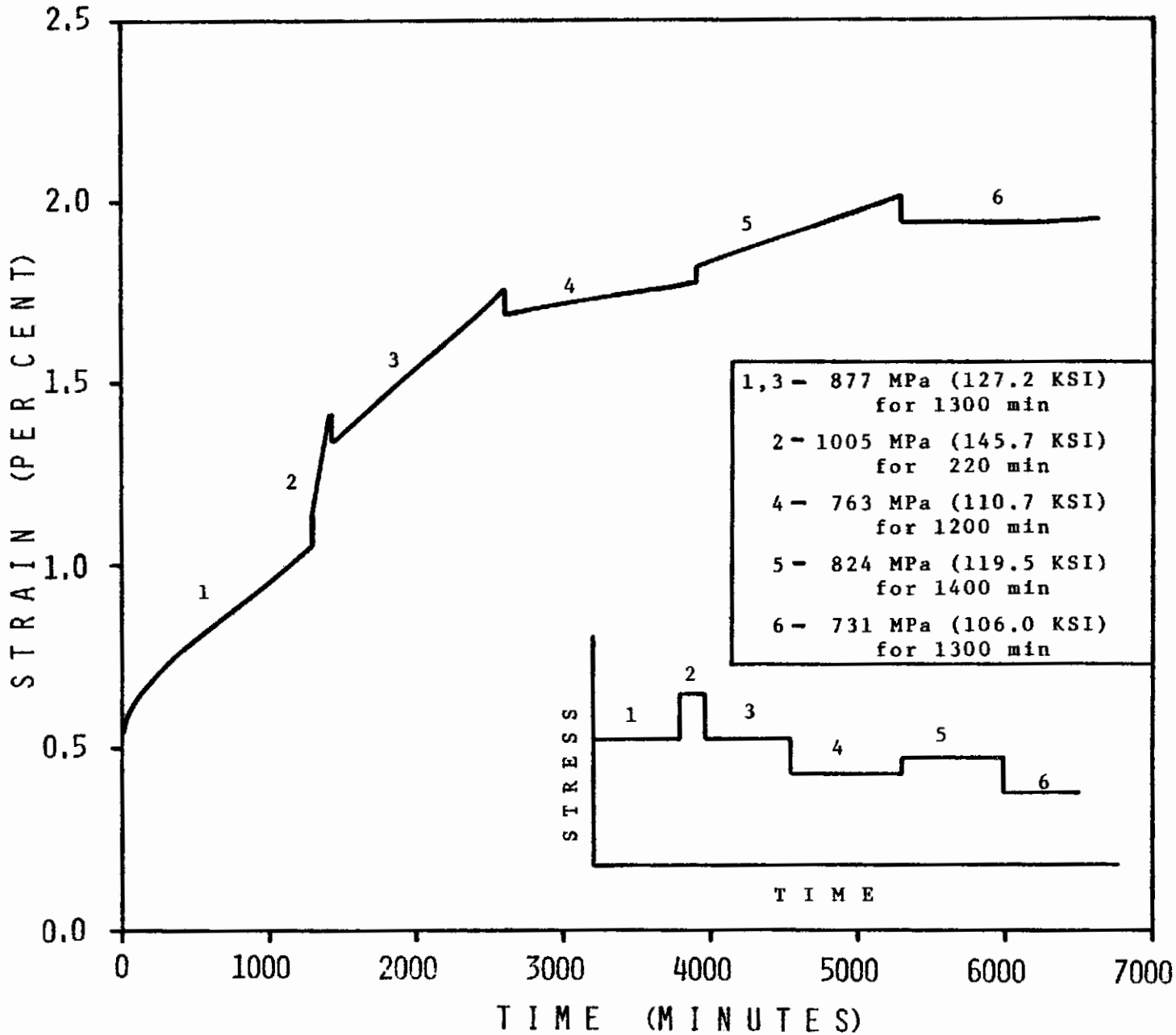

FIGURE 21 . TENSILE CREEP RESPONSE OF RENÉ 95 AT 650°C (1200°F) DUE TO A SIX STEP STRESS HISTORY (SPECIMEN 2-7)

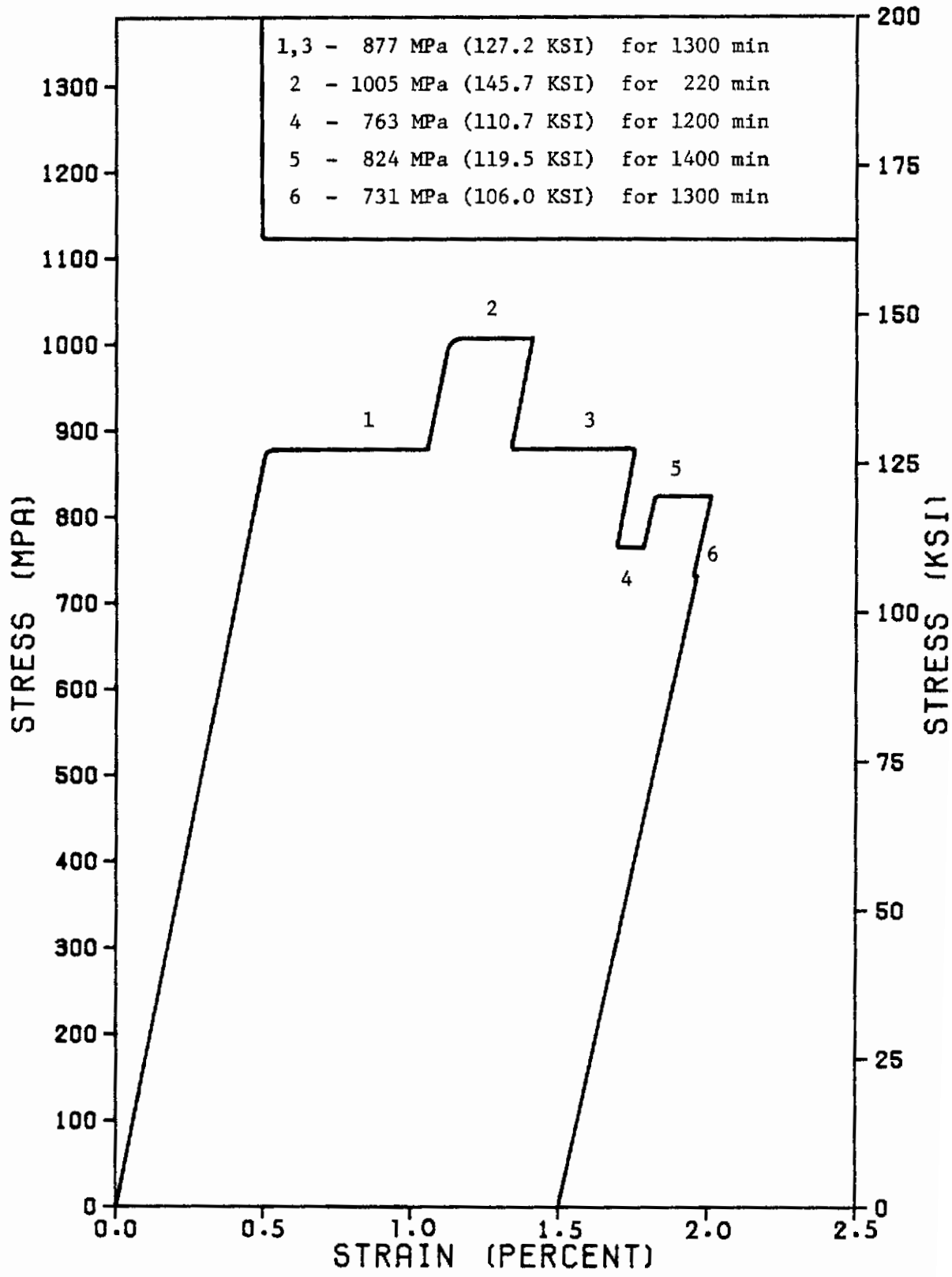

FIGURE 22 . STRESS-STRAIN RESPONSE OF SPECIMEN 2-7 DUE TO A SIX STEP STRESS HISTORY OF RENÉ 95 AT 650°C (1200°F)

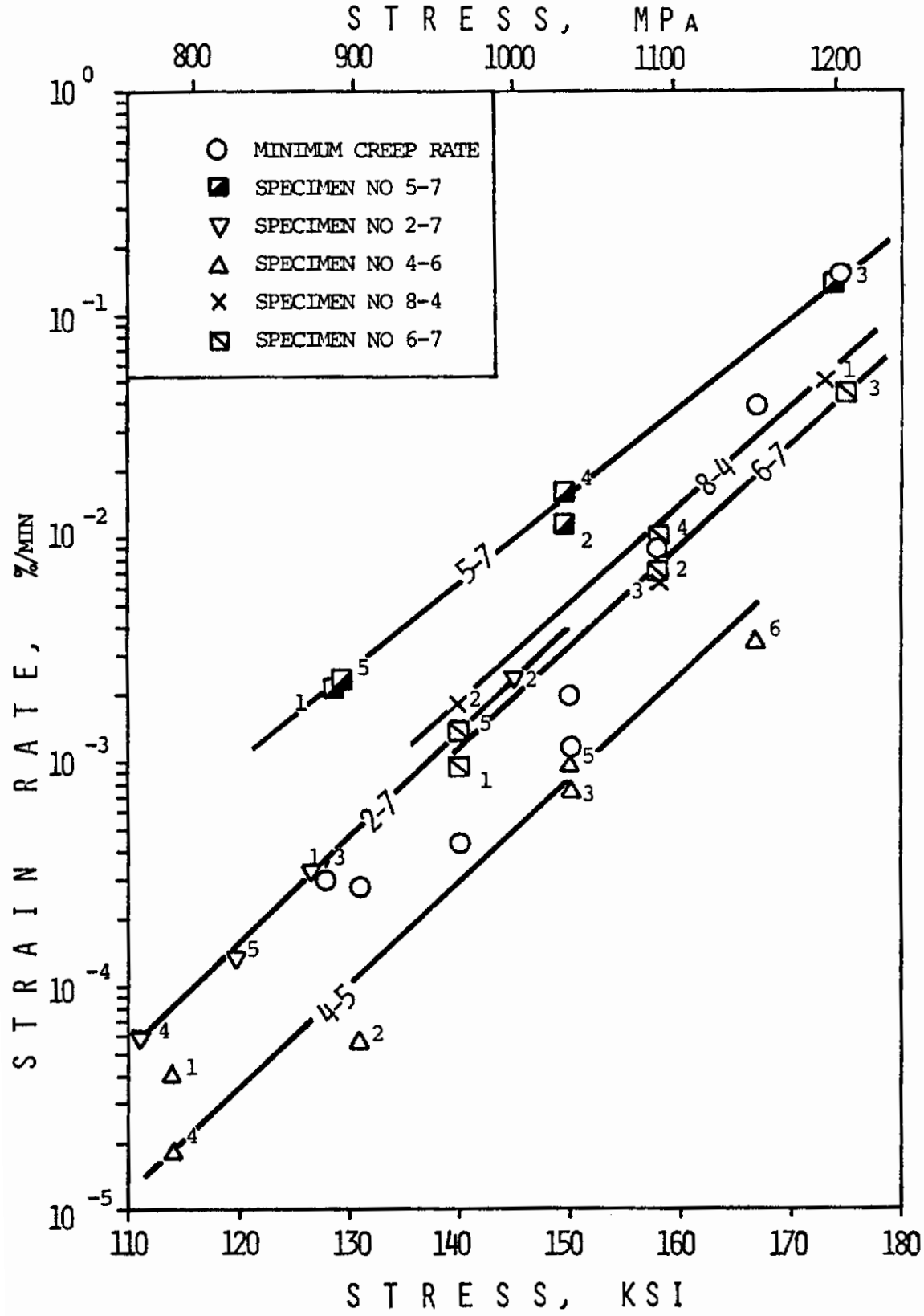

FIGURE 23. CHANGE IN AVERAGE STRAIN RATE AS A FUNCTION OF STRESS DURING A MULTY STEP CREEP TEST OF RENÉ 95 AT 650°C (1200°F).

TABLE 7. EFFECT OF TEMPERATURE ON THE CREEP RATE OF RENÉ 95 LOADED AT 1089.4 MPa (158 KSI). DATA TAKEN FROM SPECIMEN 4-5 AFTER A SIX-STEP TENSILE CREEP TEST.

SEQUENCE	TEMPERATURE ^{o}C. (^{o}F.)	DURATION MIN.	CREEP RATE %/MIN.
1	650.0 (1200)	107	1.3×10^{-3}
2	644.5 (1190)	158	1.0×10^{-3}
3	655.5 (1210)	70	2.0×10^{-3}

SECTION VII
STRESS RELAXATION AND STRAIN RECOVERY

Stress relaxation is another response characteristic that is observed in metals at elevated temperatures. This was investigated for René 95 at 650°C. (1200°F.). Specimen 5-8 was deformed to 1% strain and held at that strain for 1000 minutes. The stress relaxation response is shown in Figure 24.

Intrinsic to the material, creep and stress relaxation are observed measures of the same time characteristic, however, the roles of the independent and dependent variables are reversed. Thus, a relationship should exist between stress relaxation and creep. One of the simplest approximations of this relationship is based on the assumption of time-hardening behavior of the material, and can be established by replotting the creep data as a family of stress-strain-time (isochronous) curves as shown in Figures 25 and 26 for tension and compression, respectively. It can be seen that the isochronous curves are similar to within 2% of accuracy. This means that the creep strain can be written as separate functions of stress and time i.e.,

$$\varepsilon(t) = S(\sigma) \cdot f(t)$$

where $f(0) = 1$ is used to define the hypothetical instaneous response. In this case, as shown in Reference 23 , the stress can be expressed in the form

$$\sigma(t) = \phi(\varepsilon) \frac{1}{f(t)}$$

where the function $\phi = S^{-1}(\sigma)$ is the inverse of the function S. Thus, the intersection of a constant strain line through the family of isochronous curves represents stress relaxation. This prediction is also shown in

Figure 24. It can be seen that a reasonable correlation can be derived between creep and stress relaxation using this method; however, the initial rate of relaxation is under predicted.

The strain recovery after tensile creep was investigated at the stress levels of 1034 MPa (150 KSI) and 965 MPa (140 KSI). The specimens were subjected to a constant load for 954 min. and 2,079 min., respectively, until a strain of 2% was reached; then unloaded to very near zero stress. The recovery strain was measured for approximately 500 min. The strain recovery curves are shown in Figure 27.

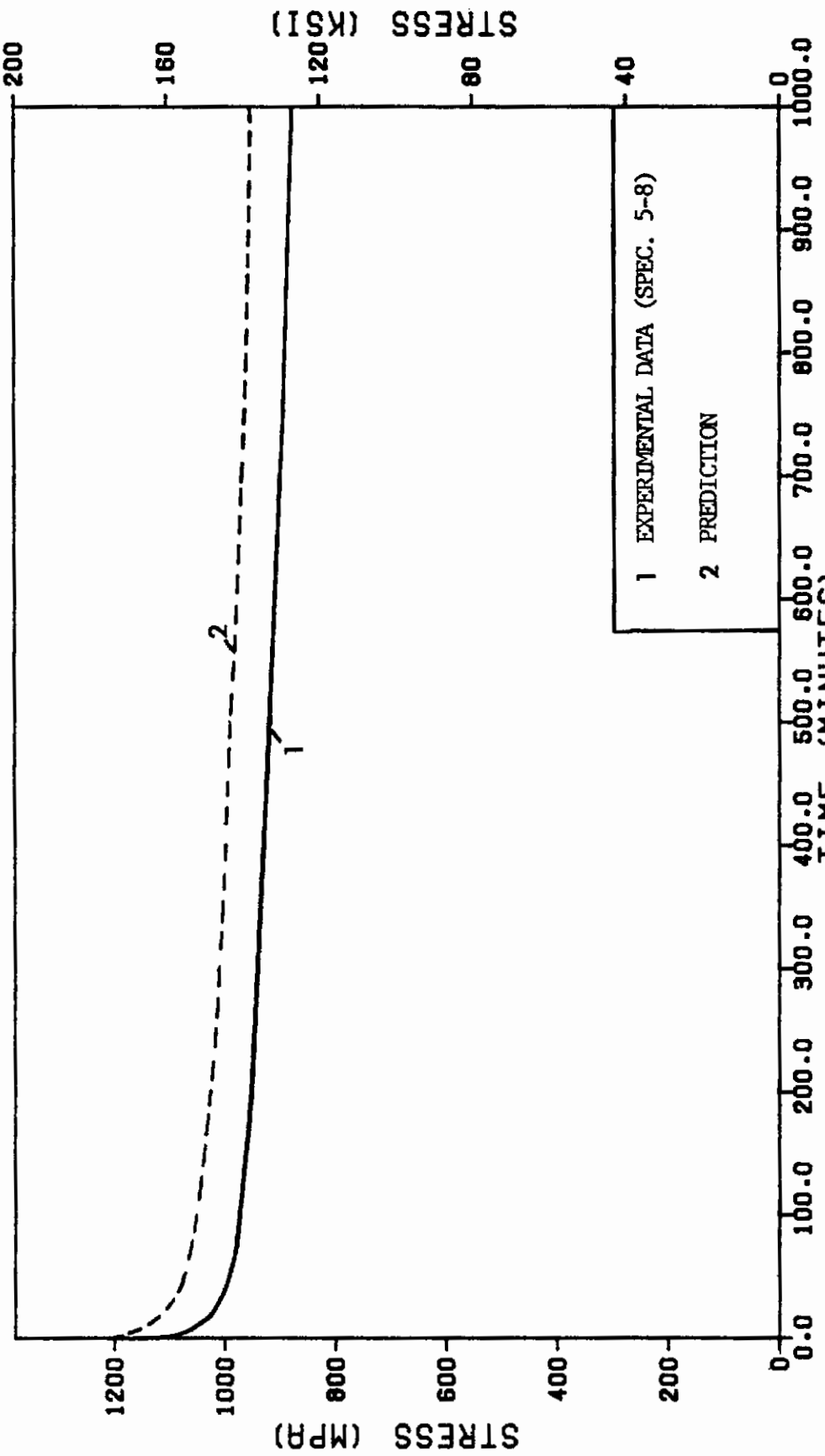

FIGURE 24. STRESS RELAXATION OF RENÉ 95 AT 650°C. (1200°F.) FOR A CONSTANT STRAIN OF 1.0% AND PREDICTED FROM THE ISOCHRONOUS CURVES.

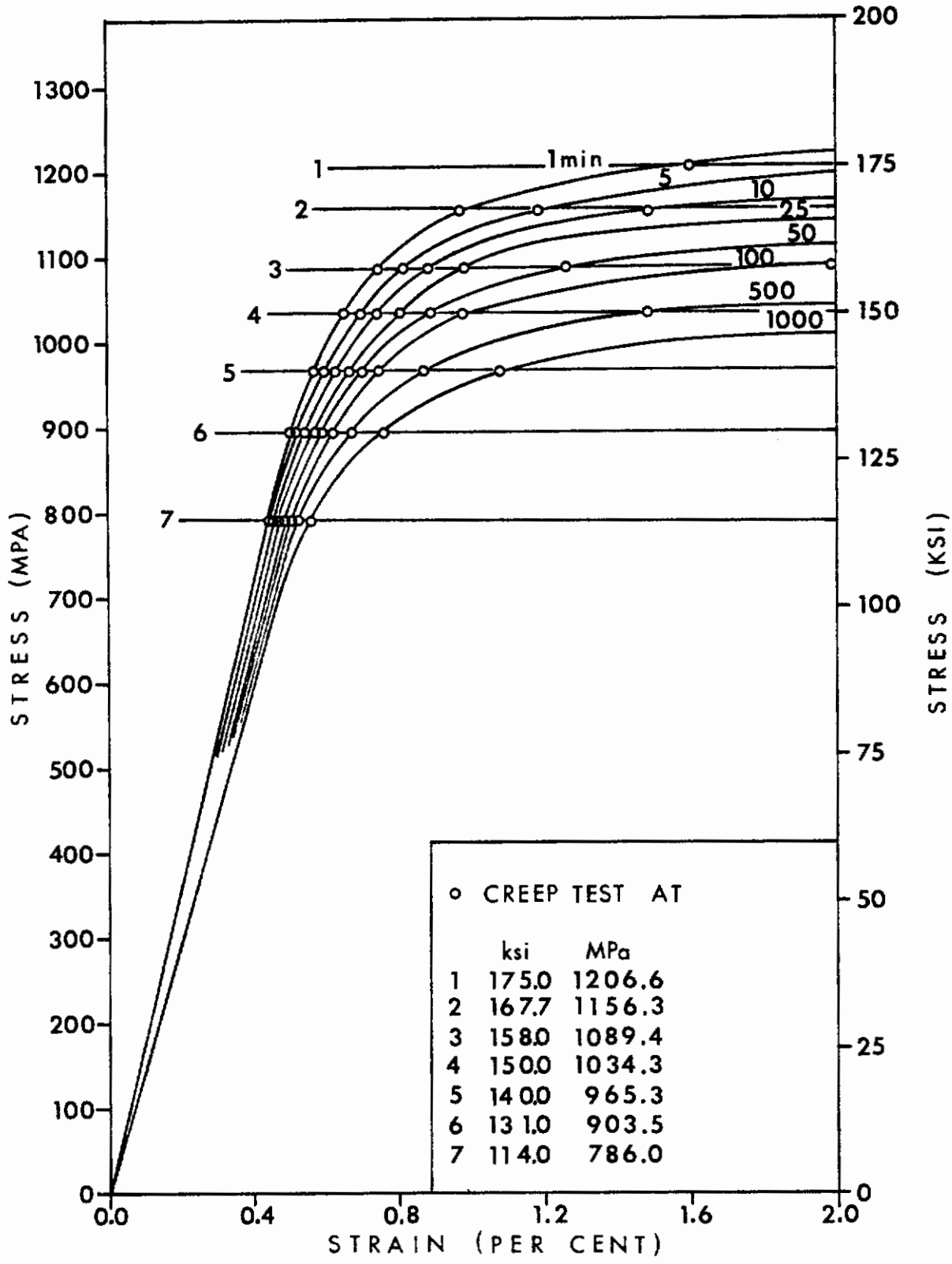

FIGURE 25. FAMILY OF ISOCHRONOUS CREEP CURVES DETERMINED FROM THE TENSILE CREEP RESPONSE OF RENÉ 95

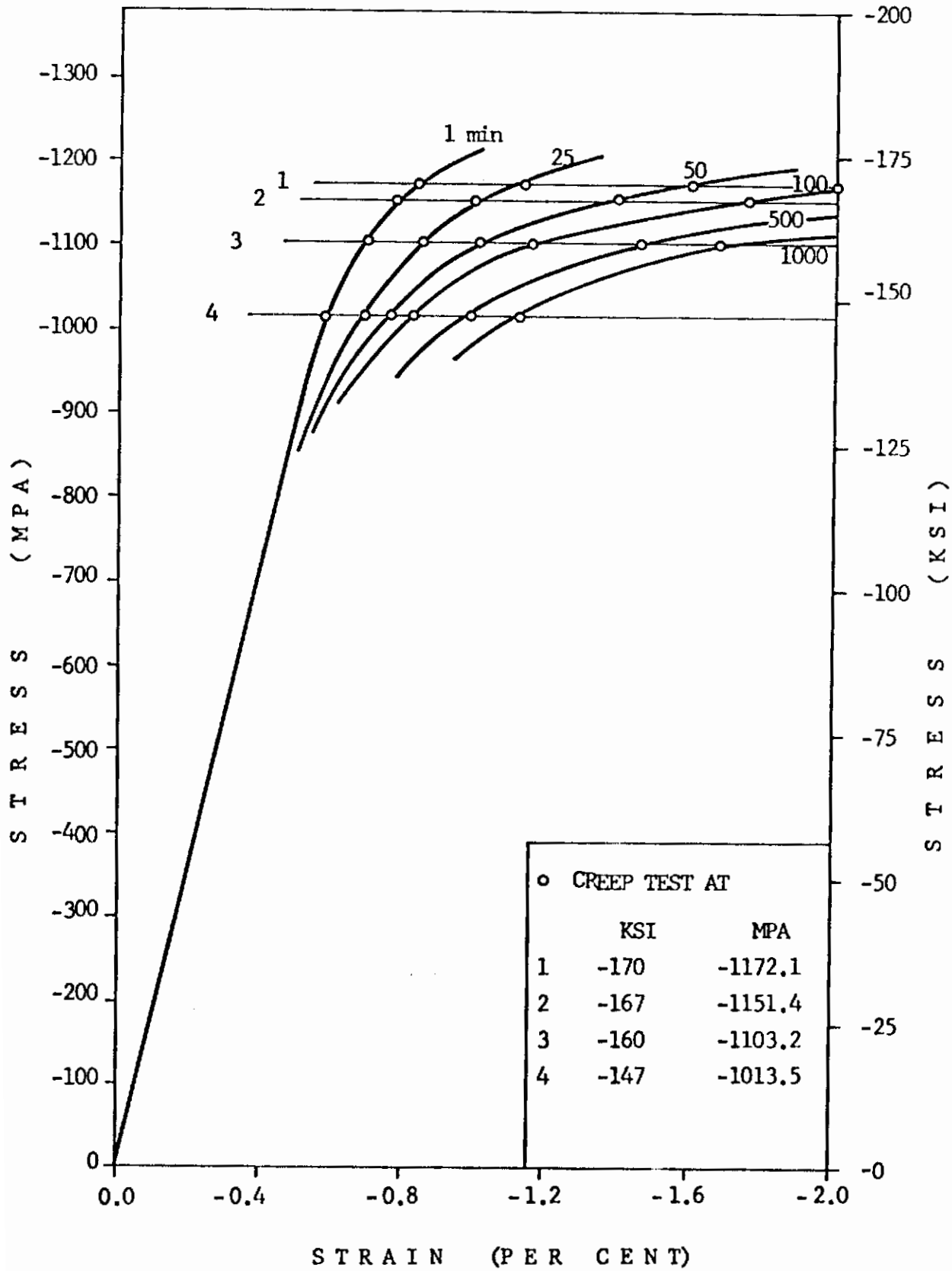

FIGURE 26. FAMILY OF ISOCHRONOUS CREEP CURVES DETERMINED FROM THE COMPRESSIVE CREEP RESPONSE OF RENÉ 95 AT 650°C (1200°F)

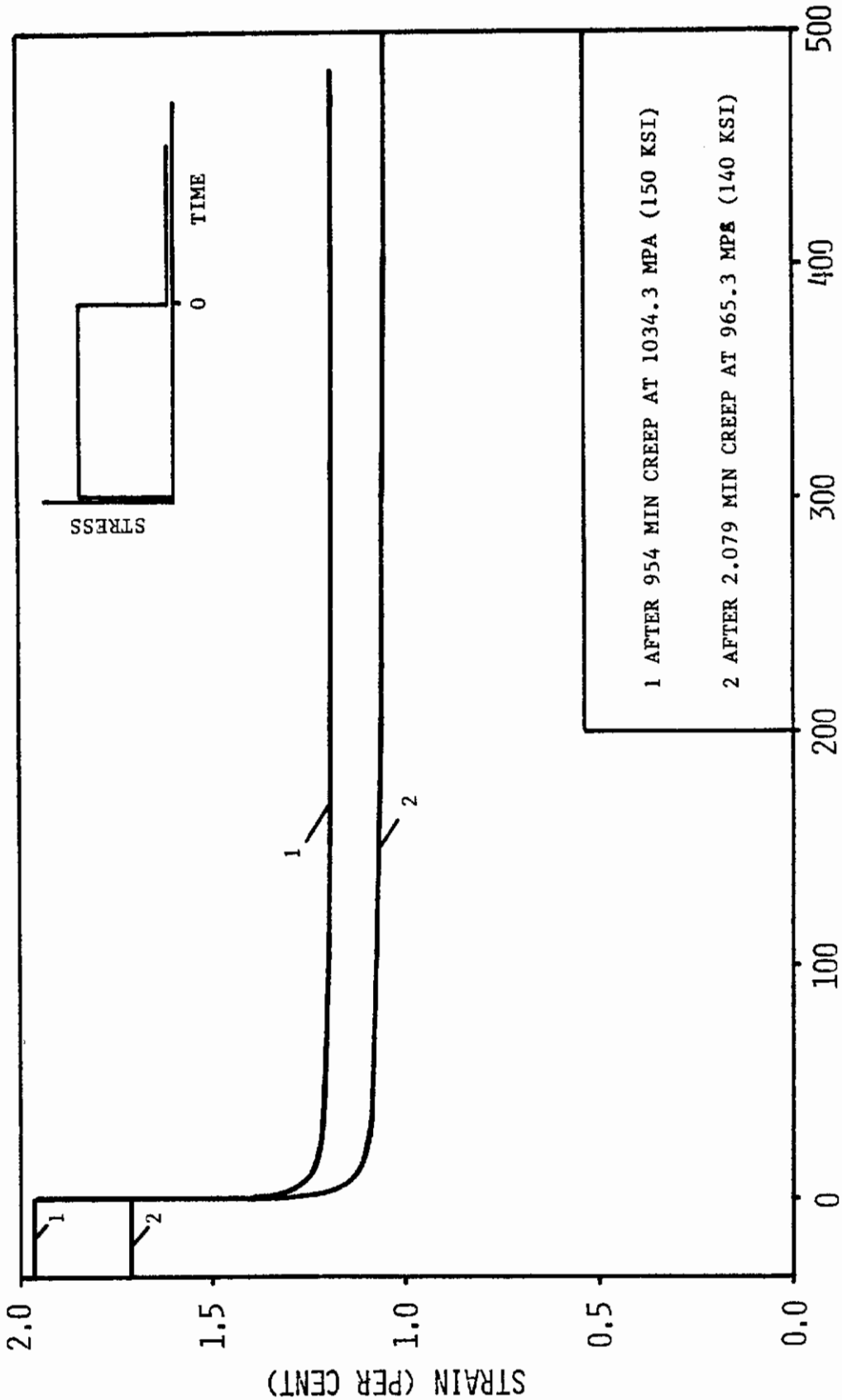

FIGURE 27. STRAIN RECOVERY AFTER TENSILE CREEP OF RENÉ 95 AT 650°C (1200°F)

SECTION VIII
FATIGUE UNDER STRESS CONTROL

The low cycle fatigue is an important property of materials that is generally not modeled well in constitutive equations. This is true when the cycle is complicated or involves periods of creep or stress relaxation. These phenomena require a thorough understanding of the creep fatigue damage coupling process and how it affects the loop geometry and life. The objective of these few tests is to begin to investigate the constitutive modeling aspects of reverse plastic flow, the prediction of the loop geometry, and their impact on the life of the specimen.

The life prediction problem for René 95 has been previously investigated by Bernstein (Reference 7). Some important observations for constitutive modeling can be drawn from this work. The hysteresis loop geometry during symmetric strain range control experiments developed a mean compressive stress. During tensile strain-hold tests, compressive mean stresses also developed; however, during compressive hold-time tests, a mean tensile stress developed that was less in magnitude than the corresponding tensile hold time tests. These observations are consistent with the fact that the time dependent compression response properties (creep and stress relaxation) are less than the tensile properties. These ideas must ultimately be included in any theory that is used to predict the response of René 95.

The experiments in this study were run under stress control to provide direct correlation with the previous creep and tensile response data. A summary of the testing program is shown in Table 8. All tests were run with $A = \infty$ except specimen 5-6. The test frequency was 10 CPM and all specimens failed in the gage section. The distribution of the life, as a function of total stress range, is shown in Figure 28. A reasonable consistency in the

life data exists. It can be seen that starting a test with the first quarter cycle in compression, specimen 5-3, did not significantly affect the life. Further, preceding the fatigue by tensile or compressive creep strain did not significantly alter the life.

The hysteresis loop geometry is dramatically changed with fatigue. To begin, the effect of hardening during the first one and one-quarter cycles can be seen in Figures 29, 30 and 31. The transition from elastic to inelastic flow is less sharp during the fifth quarter cycle than in the first quarter cycle and the amount of plastic strain is reduced. This effect produces a reduction in the amount of plastic work as a function of cycling. This also gives an apparent softening of the tangent modulus.

As shown in Figure 32, the material approaches a quasi-stable loop geometry with a mean tensile strain after about the first twenty-five cycles. However, it is clear from Figure 33 that the loop geometry does not ever stabilize during a fatigue test. After initially hardening the material softens for the duration of the test. A mean tensile strain was developed in all specimens; even specimen 5-3 that was started in compression. The development of the mean tensile strain clearly indicates that the difference in the tensile and compressive properties as discussed in Sections IV and V are important in fatigue.

The effect of prior tensile and compressive creep on the hysteresis loop geometry is summarized in Table 9. All specimens shown in Table 10 were run using a symmetric stress control range of 1930 MPa (280 KSI), developed a mean tensile strain and exhibited about the same life. The prior tensile strain of 1.70% most likely implies that specimen 4-8 is operating in a tertiary creep domain (see Figure 13), thereby giving rise to a larger inelastic strain range. The prior compressive creep strain history produced the largest inelastic

strain range, which appears to arise from the Bauschinger effect. The rate of growth of the inelastic strain range is about the same for all three specimens.

TABLE 8. LOW CYCLE FATIGUE PROPERTIES OF RENÉ 95 AT 650°C (1200°F).

SPEC. NO.	σ_{max} FIRST CYCLE MPa (KSI)	$\Delta\sigma$ MPa (KSI)	$\Delta\varepsilon$ AT START %	$\Delta\varepsilon$ NEAR $N_f/2$ %	N_f CYCLES
2-6	921 (133.6)	1842 (267.2)	1.03	1.04	3116
3-3	965 (140.0)	1930 (280.0)	1.10	1.11	1855
6-2	1051 (152.5)	2102 (304.9)	0.60	0.60	811
3-6	1092 (158.4)	2184 (316.7)	1.29	1.32	840
2-3	1127 (163.5)	2255 (327.0)	1.40	1.40	482
5-3(1)	1159 (168.1)	2317 (336.1)	-	1.61	404
4-3	1206 (175.0)	2418 (350.7)	1.86	1.66	194
4-8(2)	965 (140.0)	1930 (280.0)	-	-	2244
2-8(3)	965 (140.0)	1930 (280.0)	-	-	2316
5-6(4)	1158 (168.0)	1737 (252.0)	0.955	0.980	2435

(1) First quarter cycle in compression.

(2) Following tensile creep at ε = 1.70%.

(3) Following compressive creep to ε = -0.624%.

(4) σ_m = +290 MPa (42 KSI).

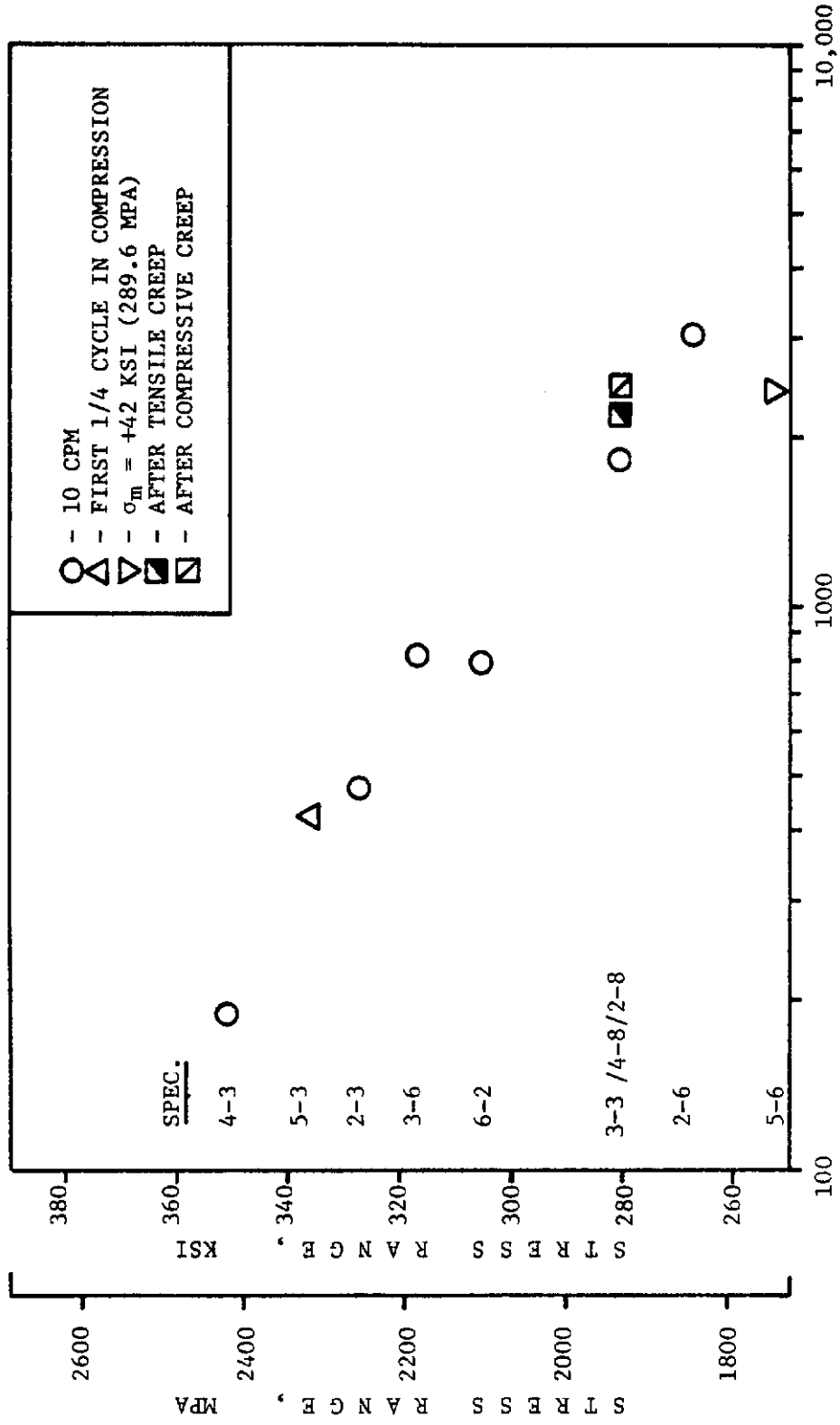

FIGURE 28. LOW CYCLE FATIGUE LIFE OF RENÉ 95 AT 650°C (1200°F) AS A FUNCTION OF TOTAL STRESS RANGE.

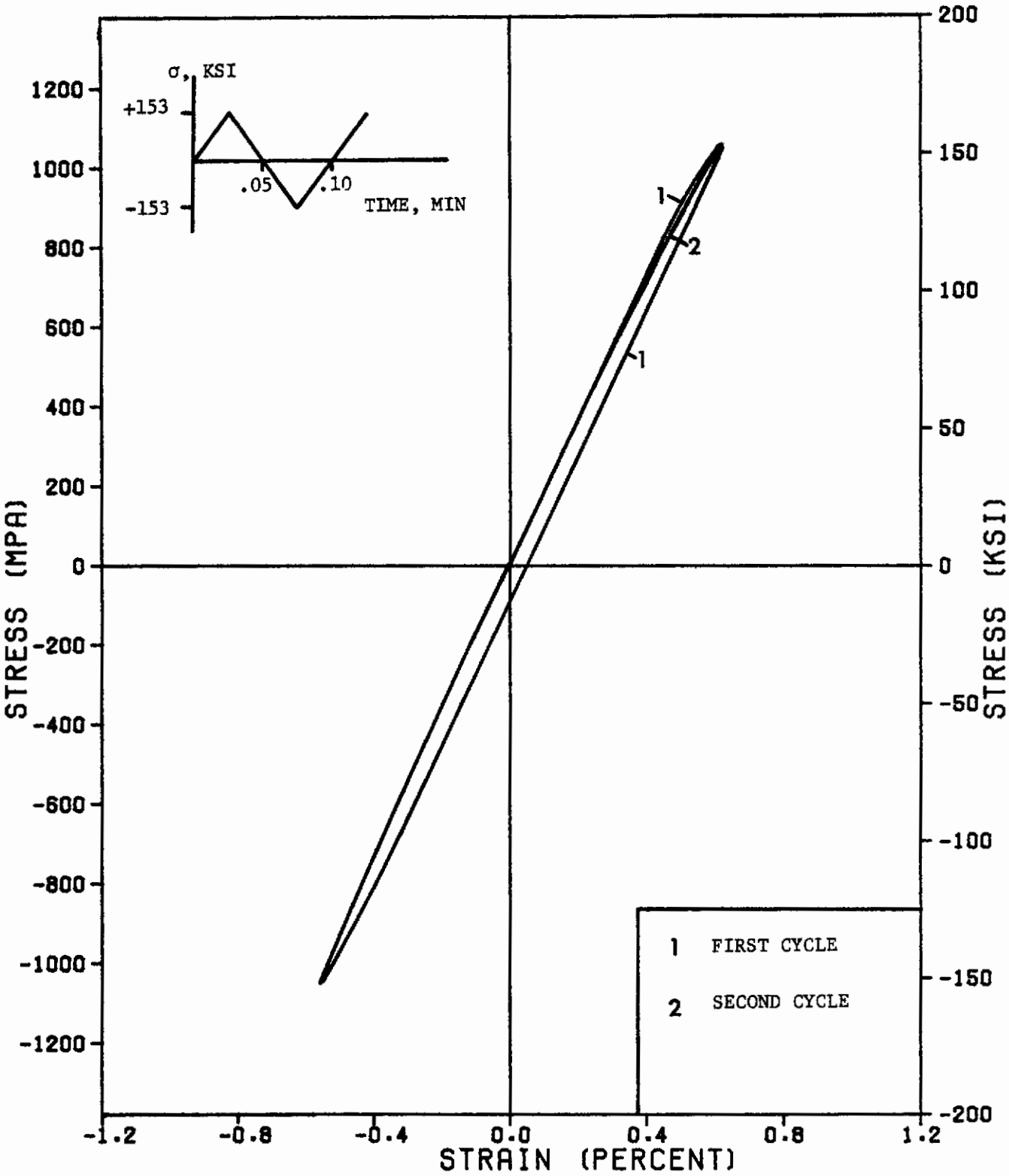

FIGURE 29. HYSTERESIS LOOP FOR RENÉ 95 AT 650°C (1200°F) FOR SPECIMEN 6-2 USING A TOTAL STRESS RANGE OF 2102 MPA (304.9 KSI)

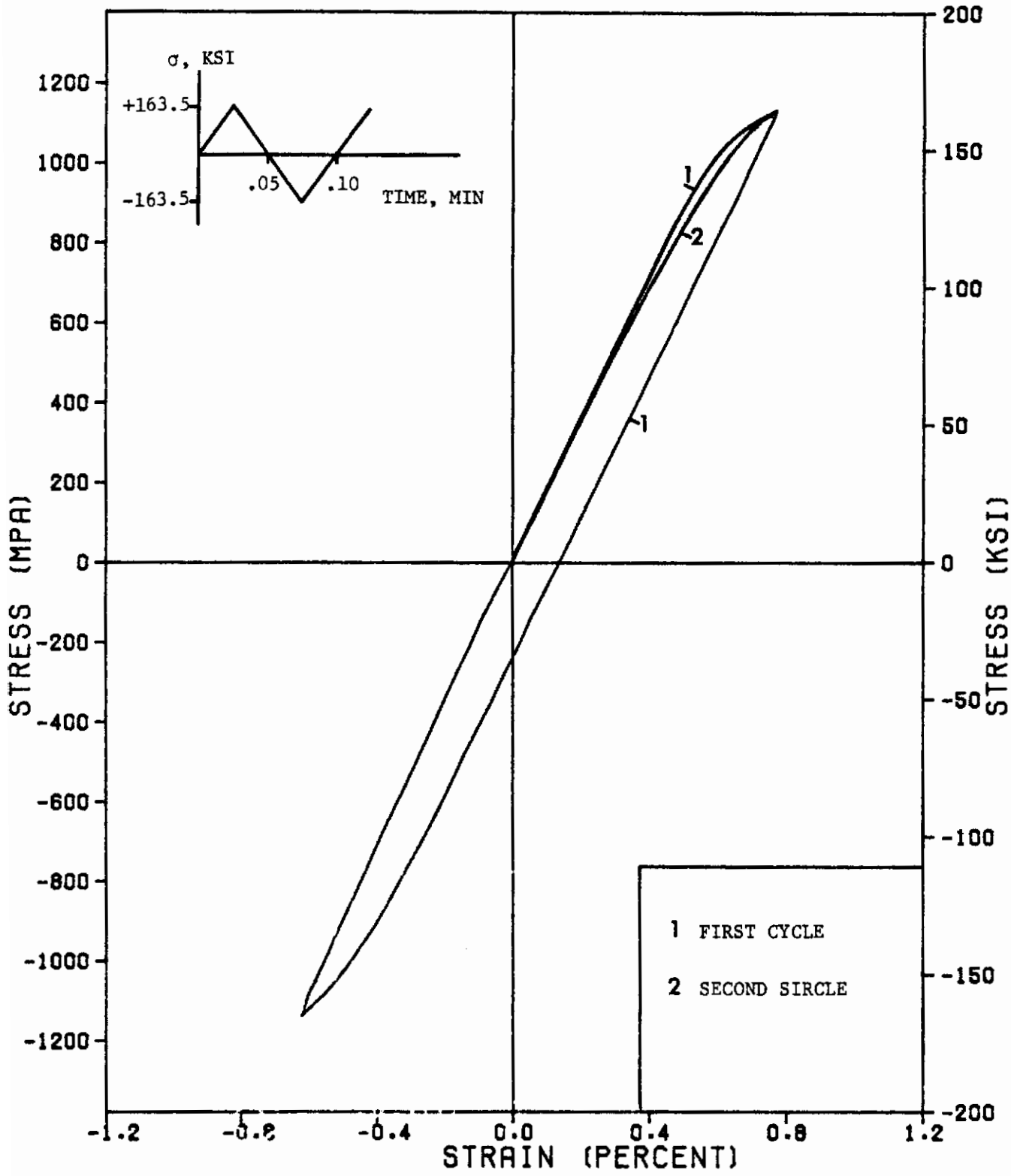

Figure 30. Hysteresis loop for René 95 at 650°C. (1200°F.) for specimen 2-3 using a total stress range of 2255 MPa (327 KSI).

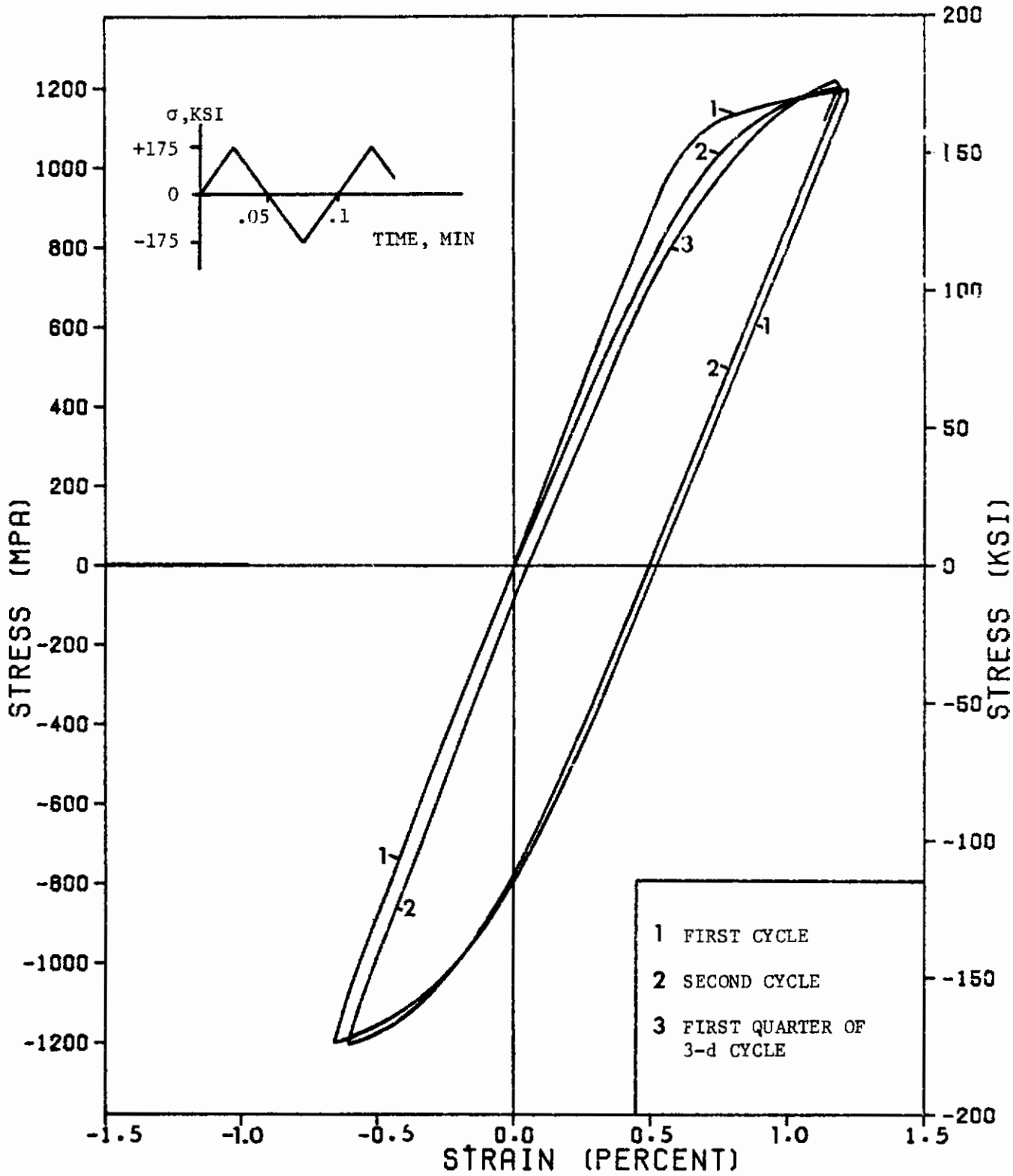

Figure 31. Hysteresis loops for René 95 at 650°C. (1200°F.) for specimen 4-3 using total stress range of 2413 MPa (350.7 KSI).

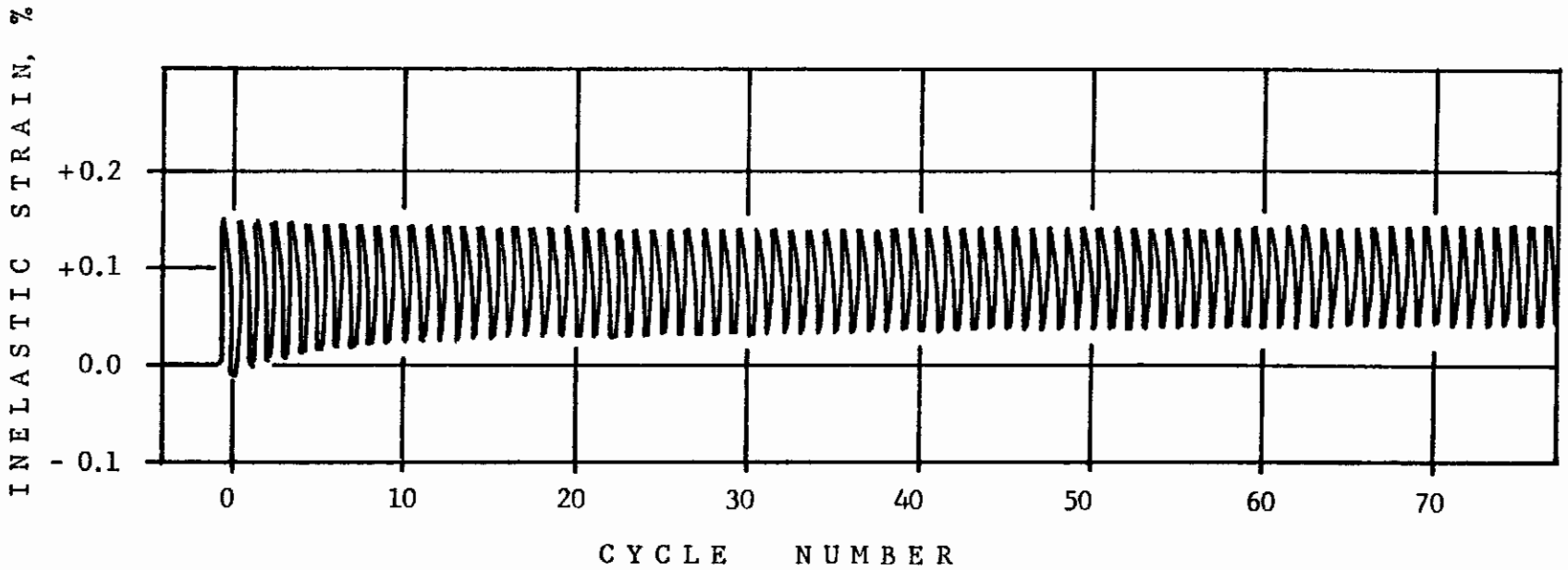

FIGURE 32. CHANGE OF INELASTIC STRAIN AS A FUNCTION OF NUMBER OF CYCLES FOR RENÉ 95 AT 650°C (1200°F). SPECIMEN 2-3 WAS STARTED IN TENSION AND CYCLED BETWEEN ±1127.3 MPa (±163.5 KSI)

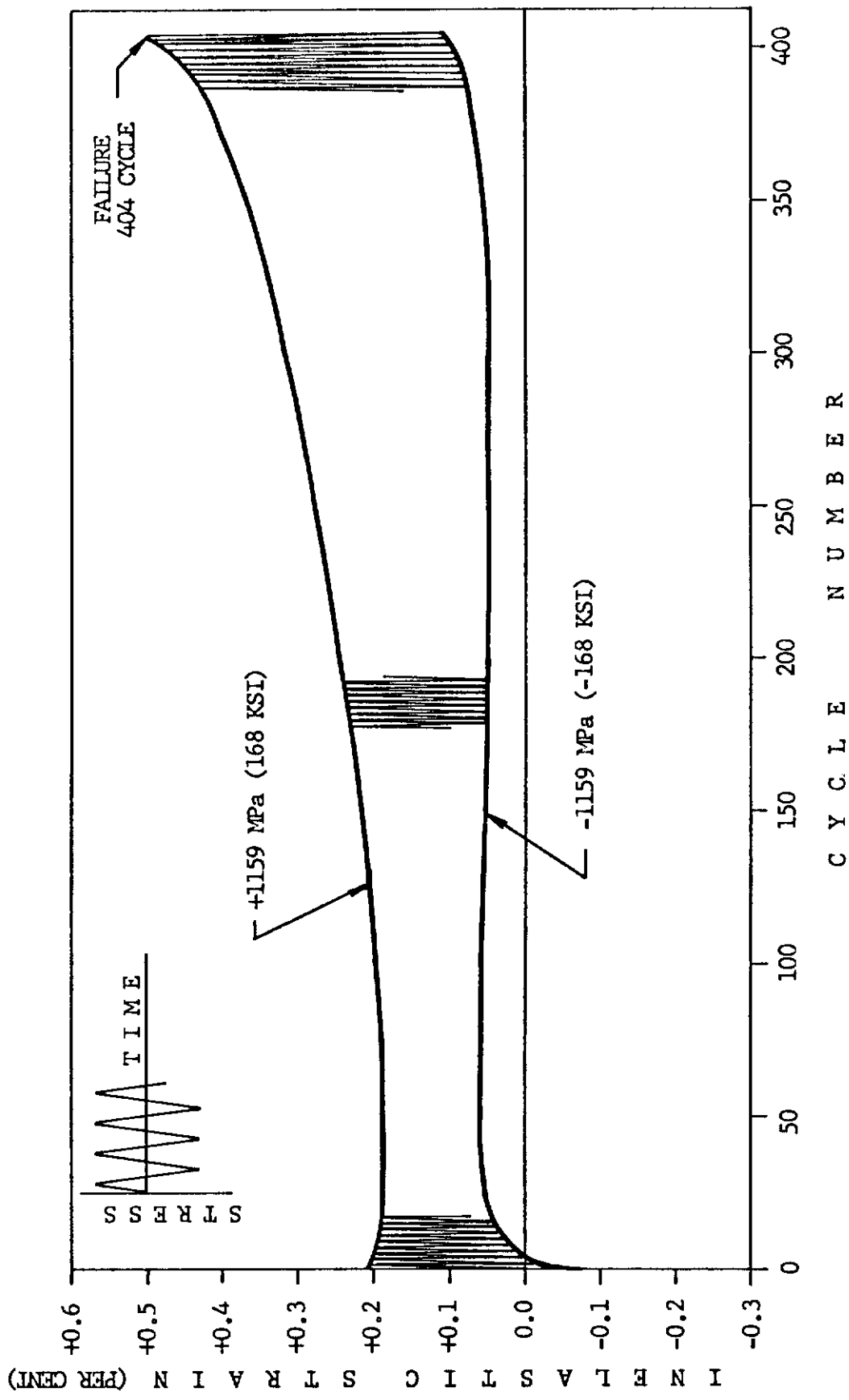

FIGURE 33. ENVELOPE OF THE INELASTIC STRAIN FOR THE ENTIRE LIFE OF THE MATERIAL. SPECIMEN 5-3 WAS STARTED IN COMPRESSION AND CYCLED BETWEEN ±1159 MPa (±168 KSI)

TABLE 9. EFFECT OF TENSILE AND COMPRESSIVE CREEP ON THE HYSTERESIS LOOP GEOMETRY OF RENE 95 AT 650°C (1200°F).

SPEC. NO. CREEP	3-3 0.0%	4-8 +1.70%	2-8 -0.624%
CYCLE NO.	$\Delta\varepsilon^I$	$\Delta\varepsilon^I$	$\Delta\varepsilon^I$
100	0.020	0.035	0.055
500	0.030	0.050	0.065
1000	0.040	0.055	0.078

SECTION IX
SUMMARY

The above set of experiments on Renė 95 at 650°C (1200°F) clearly indicates some important response trends. These tests were not fully comprehensive since compressive response was not included in the multi-step creep programs. It is also important to look at the effect of fatigue on creep, which should be more dramatic than the effect of prior creep on fatigue. Despite these absences, the following observations can be made:

(1) There is no consistent variation in response attributed to the location of the specimen blank in the Renė 95 pancake.

(2) The compressive response of Renė 95 under strain rate control is 0% - 10% stiffer than the tensile response.

(3) The minimum creep rate in tension is about one decade faster than minimum creep rate in compression at the corresponding negative stress level.

(4) The material develops a mean tensile strain in stress control fatigue tests showing the cumulative effect in fatigue of the difference in the tensile and compressive response.

(5) The ultimate stress response varies with strain rate during a stress-strain test. This rate sensitivity corresponds to the minimum strain rate in a creep test.

(6) The duration of primary creep of Renė 95 is small compared to the secondary creep region; however, the majority of the creep life is spent in tertiary creep. The minimum creep rate curve is approximately a linear function of true stress. The creep and constant strain rate tensile data can be correlated using the stress minimum creep rate curve.

(7) Step changes in the creep stress are independent of sequence (history) when the strain is in the secondary creep rate region.

(8) Stress relaxation and creep can be correlated relatively well using the isochronous creep response curves.

(9) The material demonstrates strain recovery of about 10% the total strain.

REFERENCES

[1] Menon, M. N. and Reiman, W. H., Tensile Behavior of Renė 95 in the Thermomechanically Processed and Conventionally Processed Forms" Metallurgical Transactions, 6A, 1975, pp. 1078-1085.

[2] Shamblem, C. E., Allen, R. E. and Walker, F. E., "Effect of Processing and Microstructure on Renė 95", Metallurgical Transactions, 6A, 1975, pp. 2073-2082.

[3] Menon, M. N. and Reiman, W. H., "Deformation Twins in Renė 95", Metallography, 8, 1975, pp. 221-226.

[4] Menon, M. N., "Metallographic Characterization of Renė 95 Forgings", AFML-TR-73-180 (Air Force Wright Aeronautical Laboratory, Wright-Patterson A. F. B., Ohio), 1976.

[5] Menon, M. N. and Reiman, W. H., "Low-Cycle Fatigue Crack Initiation Study in Renė 95", Journal of Materials Science, 10, 1975, pp. 1571-1581.

[6] Menon, M. N., "Life Prediction Techniques for Analyzing Creep-Fatigue Interaction in Advanced Nickel-Base Superalloys", AFML-TR-76-172 (Air Force Wright Aeronautical Laboratory, Wright-Patterson A. F. B., Ohio), 1976.

[7] Bernstein, H. L., "An Evaluation of Four Current Models to Predict the Creep Fatigue Interaction in Renė 95", AFML-79-4075 (Air Force Wright Aeronautical Laboratory, Wright-Patterson A. F. B., Ohio), 1979.

[8] Manson, S. S., Halford, G. R. and Hirschberg, M. H., Creep-Fatigue Analysis by Strainrange Partitioning, NASA TM X-67838 (NASA-Lewis Research Center, Cleveland, Ohio), 1971.

[9] Manson, S. S., "The Challenge to Unify Treatment of High Temperature Fatigue - A Partisan Proposal Based on Strainrange Partitioning", Fatigue at Elevated Temperatures, ASTM STP 520 (American Society for Testing and Materials, Philadelphia, Pennsylvania), 1978, pp. 744-775.

[10] Manson, S. S., Halford, G. R., and Hirschberg, M. H. "Strainrange Partitioning - A Tool for Characterizing High-Temperature, Low-Cycle Fatigue", NASA TMS-71691 (NASA-Lewis Research Center, Cleveland, Ohio), 1975.

[11] Coffin, L. R., Jr., "The Concept of Frequency Separation in Life Prediction for Time-Dependent Fatigue", in 1976 ASME-MPC Symposium on Creep-Fatigue Interaction, MPC-3 (American Society of Mechanical Engineers, NY), 1976, pp. 349-364.

[12] Time Dependent Fatigue of Structural Alloys, ORNL-5073 (Oak Ridge National Laboratory, Oak Ridge, Tennessee), 1975, pp. 109-133.

[13] Ostergren, W. J. "A Damage Function and Associated Failure Equations for Predicting Hold Time and Frequency Effects in Elevated Temperature, Low Cycle Fatigue", ASTM Standardization News 4.10 pp. 327, 1976.

[14] Ostergren, W.J., "Correlation of Hold Time Effects in Elevated Temperature Low Cycle Fatigue Using a Frequency Modified Damage Function", 1976 ASME-MPC Symposium on Creep-Fatigue Interaction, MPC-3 (American Society of Mechanical Engineers, New York), 1976, pp. 179-202.

[15] Majumdar, S. and Maiya, P. S., "A Unified and Mechanistic Approach to Creep Fatigue Damage", ANL-76-58 (Argonne National Laboratory, Argonne, Illinois), January 1976.

[16] Majumdar, S. and Maiya, P. S., "A Damage Equation for Creep-Fatigue Interaction", 1976 ASME-MPC Symposium on Creep-Fatigue Interaction, MPC-3 (American Society of Mechanical Engineers, New York), 1976, pp. 323-336.

[17] Majumdar, S. and Maiya, P. S., "Wave Shape Effects in Elevated-Temperature Low Cycle Fatigue of Type 304 Stainless Steel", in Inelastic Behavior of Pressure Vessle and Piping Components, PVP-PB-028 (American Society of Mechanical Engineers, New York), 1978, pp. 43-54.

[18] Stouffer, D. C., "An Evaluation of the Monotonic Response of René 95 at 1200°F.", AFOSR-TR-78-0905 (Air Force Office of Scientific Research, Bolling A. F. B., D. C.), 1978.

[19] Plumbridge, W. J. and Miller, K. J., "Influence of Prior Fatigue of the Creep of a Non-Heat Treated Alloy Steel", Metals Technology, 169, 1975, pp. 249-252.

[20] Bodner, S. R. and Partom, Y. "Constitutive Equations for Elastic-Viscoplastic Strain Hardening Materials", Journal of Applied Mechanics, 42, 1975, pp. 385-389.

[21] Bodner, S. R., "Representation of Time Dependent Mechanical Behavior of René 95 by Constitutive Equations", AFML-TR-79-4116 (Air Force Wright Aeronautical Laboratory, Wright Patterson A. F. B., Ohio), 1979.

[22] Antolovich S. D., Baur R. and Liu S. "A Mechanistically Based Model of High Temperature L.C.F. of NI Base Super alloys". Department of Material Science, University of Cincinnati, Cincinnati, Ohio, 1980.

[23] Rabotnov, Y. N., Creep Problems in Structural Members, North Holland, 1969.

☆U.S.Government Printing Office: 1980 — 757-002/275